~~RESTRICTED~~

COPY NO. 133
RM No. E8C16

NACA

RESEARCH MEMORANDUM

STUDY OF STRESS STATES IN GAS-TURBINE DISK AS DETERMINED FROM MEASURED OPERATING-TEMPERATURE DISTRIBUTIONS

By J. Elmo Farmer, M. B. Millenson
and S. S. Manson

Flight Propulsion Research Laboratory
Cleveland, Ohio

NATIONAL ADVISORY COMMITTEE
FOR AERONAUTICS

WASHINGTON

July 21, 1948

~~RESTRICTED~~

National Aeronautics and
Space Administration

Langley Research Center
Hampton, Virginia
23665

Reply to Attn of 139A

JUN 16 1983

TO: Distribution

FROM: 180A/Security Classification Officer

SUBJECT: Authority to Declassify NACA/NASA Documents Dated Prior to January 1, 1960

Effective this date, all material (informal, correspondence) classified by this Center prior to January 1, 1960, is declassified. This action does not include material derivatively classified at the Center upon instructions from other Agencies.

Immediate re-marking is not required; however, until material is re-marked by lining through the classification and annotating with the following statement, it must continue to be protected as if classified:

> "Declassified by authority of LaRC Security Classification Officer (SCO) letter dated June 16, 1983," and the signature of person performing the re-marking.

If re-marking a large amount of material is desirable, but unduly burdensome, custodians may follow the instructions contained in NHB 1640.4, subpart F, section 1203.604, paragraph (h).

This declassification action complements earlier actions by the National Archives and Records Service (NARS) and by the NASA Security Classification Officer (SCO). In Declassification Review Program 807008, NARS declassified the Center's "Research Authorization" files, which contain reports, Research Authorizations, correspondence, photographs, and other documentation. Earlier, in a 1971 letter, the NASA SCO declassified all NACA/NASA formal series documents with the exception of the following reports, which must remain classified:

Document No.	First Author
E-51A30	Nagey
E-53G20	Francisco
E-53G21	Johnson
E-53K18	Spooner
SL-54J21a	Westphal
E-55C16	Fox
E-56H23a	Himmel

JUN 23 1983

If you have any questions concerning this matter, please call Mr. William L. Simkins at extension 3281.

Jess G. Ross
2898

Distribution:
SDL 031

cc:
NASA Scientific and Technical
Information Facility
P.O. Box 8757
BWI Airport, MD 21240

NASA--NIS-5/Security
180A/RIAD
139A/TU&AO
139A/WLSimkins:elf 06/15/83 (3281)
139A/JS 6-15-83

31-01 HEADS OF ORGANIZATIONS
HESS, JANE S.,
MAIL STOP 185 BLDG 1194

NACA RM No. E8C16 [redacted]

NATIONAL ADVISORY COMMITTEE FOR AERONAUTICS

RESEARCH MEMORANDUM

STUDY OF STRESS STATES IN GAS-TURBINE DISK AS DETERMINED FROM MEASURED OPERATING-TEMPERATURE DISTRIBUTIONS

By J. Elmo Farmer, M. B. Millenson
and S. S. Manson

SUMMARY

Results are presented of an experimental investigation to determine the temperature distribution in an aircraft-engine gas-turbine disk. High axial- and radial-temperature gradients were found to exist both when the engine was accelerated as rapidly as possible to maximum speed and power output and when it was gradually brought to these conditions in a manner typical of normal service operation. Calculated stresses based on the measured temperature distributions are presented.

Calculations based on the temperature distributions of the cooled and of the uncooled faces of the disk indicate the desirability of operating with a low degree of inner-region cooling, particularly in disks with welded blades.

INTRODUCTION

The stresses in a gas-turbine disk are significantly affected by the temperature gradients that exist within it. The rim, which is close to the hot gases, operates at a high temperature. The inner region, whose radius is less than two-thirds the rim radius, is usually much cooler because of its remoteness from the hot gases and also because of its proximity to a roller or journal bearing that must be maintained at a low operating temperature. The resultant tendency towards differential thermal expansion of the various regions produces a system of thermal stresses, which sometimes constitute the predominant stresses in the disk. In the inner region, these thermal stresses are tensile and they aggravate

the severity of the stress state by adding to the centrifugal tensile stresses; at the rim they are compressive and may, under severe conditions, produce compressive plastic flow. In disks that have essentially continuous rims, such as those with welded blades, the plastic flow may result in residual tensile stresses and ultimately in the initiation and propagation of cracks between the bases of the blades. Before the complete stress system can be determined, therefore, the thermal stresses must be investigated. Because of the lack of data on actual temperature distributions during service operation of gas-turbine disks, however, the accurate calculation of the thermal stresses and their effect on the severity of the stress state in the disk has heretofore been impossible.

An investigation of the most severe operating-temperature conditions to which a turbine disk is subjected and the stresses present at these operating conditions was therefore conducted at the NACA Cleveland laboratory. The temperatures were measured by means of rotating thermocouples (reference 1) and the operating stresses were calculated by the methods of references 2 and 3.

One face of the inner region of the disk is subjected to cooling air and the other face is subjected to the leakage of hot gases. A comparison between the temperature distributions on the two faces was used to derive qualitative conclusions on the desirability of inner-region turbine-disk cooling, based on its effect on the stresses both at the inner region of the disk and at the rim. Stress calculations were also made on a hypothetical disk similar to the one used in making the temperature measurements but having welded blades.

TEMPERATURE DETERMINATIONS

Apparatus and procedure. - A single-stage turbine wheel having an outside disk diameter of approximately 18 inches was used for this investigation. Vanes for circulating cooling air over the rear turbine bearing were machined on the upstream face of the disk. The turbine disk was of an alloy having a nominal composition of 16 Cr, 25 Ni, 6 Mo, and 0.15 C, with the balance principally Fe. The blades were of the tightly fitted fir-tree type.

The turbine wheel was installed in a turbojet engine having a dual-entry centrifugal compressor and a combustion-chamber assembly consisting of 14 individual burners. The engine was mounted on a pendulum-type sea-level test stand, as shown in figure 1.

Chromel-alumel thermocouples were located on the turbine disk as shown in figure 2. The manner in which the thermocouple lead wires were attached to the rear side of the turbine disk and to the terminal ring is shown in figure 3. The lead wires were passed through holes in the turbine and compressor shafts to copper slip rings and brushes mounted on the accessory case. The instrumentation is described in detail in reference 1.

Because of the limitation imposed by the slip-ring assembly, only six thermocouples could be connected for each run; it was therefore necessary to repeat each test condition three times to obtain all the data. Thermocouple 1 (fig. 2) on the rim was chosen as a reference and was connected during all the runs. The tail-pipe-gas temperature, which was measured by bare chromel-alumel thermocouples, was adjusted by means of a variable-area tail-pipe nozzle (fig. 1) to control conditions during the various runs. The maximum variation of temperature of the reference thermocouple between the runs occurred during the periods of acceleration. After the first 6 minutes of operation, the variation was less than 60° F. Turbine-rotor speed was measured by a chronometric tachometer.

Two types of run were made. The first was a run to simulate a typical normal take-off of an airplane powered by a turbojet engine and will be designated the typical take-off sequence. The engine was started in about 1 minute and then idled at a rotor speed of 4000 rpm for 4 minutes, which corresponds to the time during which the pilot would check the instruments. The rotor speed was increased to 7000 rpm for 4 minutes to allow the airplane to be taxied to the end of the runway. This 4-minute period was followed by a 2-minute idling period, simulating a wait for control-tower clearance. The engine was accelerated to 11,500 rpm for take-off and was held at that speed for about 15 minutes. The second type of run, designated the emergency take-off sequence, was one in which the engine was started and the rotor speed was increased as rapidly as possible without exceeding allowable gas temperatures to 11,500 rpm and was held constant at that speed. In both types of run, disk temperatures were recorded during the entire sequence.

Results of temperature measurements. - The manner in which the various parts of the disk were heated during each of the two types of run is shown in figures 4 and 5. On the upstream face of the disk, which is subjected to the cooling air, the temperature in the inner region is relatively low; whereas on the downstream face, which is uncooled and may in fact be heated by leakage of combustion gas, the inner region reaches relatively high temperatures. The discontinuity in the data presented in figures 4 and 5 is due to difficulties with the thermocouple instrumentation.

Plots of the radial temperature distributions are shown in figure 6. In figure 6(a), the temperature distributions on the cooled and uncooled faces, as well as those in the central plane of the disk, are presented for periods of 10, 12, 14, 16, and 22 minutes after the start of the typical take-off sequence. These periods give a sufficient range of time for a determination of all the most severe stress conditions. The maximum radial temperature gradient was measured on the cooled face of the disk and was about 1050° F. The axial temperature gradient was greatest near the center and was about 600° F. Figure 6(b) shows the temperatures on the two faces and the central plane 2, 4, 10, and 20 minutes after start of the emergency take-off sequence.

STRESS DETERMINATIONS

A method for calculating the stresses in a gas-turbine disk for given values of speed and temperature distribution is presented in references 2 and 3. In order to obtain accurate stress determination by this method, the temperature at any radius should be essentially uniform through the thickness of the disk. For rigorous application when a high axial thermal gradient exists, the method would have to be modified. Such modification results, however, in considerable mathematical complication. A simpler approach, which is believed to give results sufficiently accurate for engineering use, is to assume a uniform axial temperature distribution equal to that existing in the central plane of the disk. The radial temperature distribution in this central plane is therefore used in the stress equations to determine a first approximation of the gross stress distribution in the disk. In calculating the stress distributions, the holes drilled for convenience in measuring the temperatures have been neglected. Assumptions were made that the measured temperature distributions are the same as those in a solid disk under the same operating conditions.

It must be recognized, however, that because of the presence of the axial temperature gradient, the stresses are nonuniform across the thickness of the disk. In the extreme case, each face may be considered as acting independently of the remainder of the disk, and hypothetical stress determinations may be made using the radial temperature distributions at each face. If, for instance, the temperature of the cooled face of the disk is assumed to be representative of that present throughout the thickness of a disk that is cooled on both faces and the temperature on the uncooled face of the disk is assumed representative of that present throughout the thickness of a completely uncooled disk, then calculations based

on each temperature distribution will yield a basis for qualitative evaluation of the desirability of inner-region cooling. Calculations were therefore made of the stress distribution corresponding to the temperature distributions on each of the faces of the disk.

Elastic stresses. - The first step in the determination of the true state of stress in a disk is the calculation of the elastic stresses. These calculations are based on the assumption of proportionality between stress and strain. If the calculated elastic stresses at the various radii do not exceed the proportional elastic limit of the disk material at the corresponding operating temperatures, then these stresses are indeed the true operating stresses. If at any radius the proportional elastic limit is exceeded, then plastic flow takes place at this location, and the stress will be altered here and in the rest of the disk.

In addition to acting as a criterion for the presence of plastic flow and as a first step in the determination of the amount of plastic flow, the elastic stresses may be used as a basis for comparison of the severity of a number of alternative stress conditions. If the elastic stresses in one condition are greater than those of another, then the first condition may be considered more severe than the second.

The approximate stresses due to centrifugal action alone at the rated maximum speed of 11,500 rpm are presented in figure 7 so that the thermal stresses may later be evaluated by comparison. At any other speed, the stresses vary from these proportionally to the square of the speed. Actually, at this speed, the centrifugal stresses at different operating-temperature distributions differ slightly from those of figure 7 because of the variation of the physical properties, such as elastic modulus, with temperature. Such variations in physical properties are inherently taken into account in the calculation of the stresses by the method of reference 2.

The total elastic stresses, centrifugal plus thermal, for each of the temperature distributions shown in figure 6 are presented in figures 8 and 9. The elastic stresses for the temperature distributions corresponding to the central plane and the cooled and the uncooled faces of the disk for the typical take-off sequence are shown in figure 8. Figure 9 shows the corresponding elastic stresses for the emergency take-off sequence.

Plastic stresses. - The elastic stresses near the rim exceed, in the more severe cases, the elastic limit of the material during both the emergency and typical take-off sequences. Plastic flow is therefore indicated in these cases. The stresses for each case, taking into account plastic flow (reference 3) are shown in figures 10 and 11. The stresses in the rim region are relieved by the plastic flow, and the stresses at other locations in the disk are very slightly decreased by the plastic flow of the rim region.

DISCUSSION OF RESULTS

Stresses in inner region of disk. - In interpreting the elastic stresses in the inner regions, two criterions have been considered, namely, proximity to plastic flow and proximity to rupture. In order to establish such criterions, the effect of the biaxial stress condition existing throughout the disk must first be postulated. For the present purpose, it is sufficient to consider, in accordance with the distortion-energy theory, that a biaxial stress condition consisting of the two principle stresses, radial stress σ_r and tangential stress σ_t is equivalent to a condition of uniaxial stress σ_e given by

$$\sigma_e = \sqrt{\sigma_r^2 - \sigma_r \sigma_t + \sigma_t^2} \qquad (1)$$

The ratio σ_y/σ_e, where σ_y is the proportional elastic limit of the material (reference 3) at the operating temperature at any given location, is taken as a measure of the proximity of the material at this location to plastic flow. The higher the value of the ratio, the less is the probability of plastic flow. The values of this ratio for each of the three temperature distributions corresponding to the cooled and uncooled faces and the central plane are shown in figure 12(a) for 16 minutes after the start of the typical take-off sequence and in figure 12(b) for 10 minutes after the start of the emergency take-off sequence. In the inner region, from 0 to about the 6-inch radius, the ratio is greater than unity for all three temperature distributions and both take-off sequences, which indicates that no plastic flow should take place in this region. The factor is much higher for the temperature distribution at the uncooled face, which shows that if the entire thickness of the disk were operated at the temperatures that were present only on the uncooled side, the probability of plastic flow would be less than in the cases corresponding to temperatures on the cooled face or the central plane.

The reason for the lessened probability is that the low temperature gradients in the uncooled face result in low thermal stresses. The temperatures in the inner region of the disk are high, but the proportional elastic limit of this high-temperature alloy changes inappreciably below 800° F, hence the ratio σ_y/σ_e is high.

The proximity to rupture of each location in the disk is ascertained by establishing the ratio σ_2/σ_e as a criterion, where σ_2 is the estimated 2-hour stress-rupture value corresponding to the temperature existing at any particular location. The 2-hour stress-rupture value was selected because the length of time the disk is at the most severe stress condition for the inner region, represented by 16 minutes for the typical sequence and 10 minutes for the emergency sequence, is only 1 or 2 minutes for each take-off. The use of the 2-hour stress-rupture value therefore represents a comparison for 300 to 500 hours of engine operation. This ratio is also plotted for the corresponding stresses and temperature distributions at the two faces and in the central plane of the disk at the end of 16 minutes of the typical take-off sequence (fig. 12(a)) and at the end of 10 minutes of the emergency take-off sequence (fig. 12(b)). For radii of less than 6 inches, the ratio is greater than 2 for all three temperature conditions in both sequences. The temperature distribution corresponding to the uncooled face of the disk is again seen to result in a higher safety factor because the reduced gradient reduces the operating stresses more than the increased temperature decreases the strength of the material.

A comparison of figures 12(a) and 12(b) shows that the emergency take-off sequence results in only slightly more severe stress conditions than the typical take-off sequence. This slight difference in stress conditions is further demonstrated by comparison of the stress distributions for the emergency sequence shown in figure 11 with those for the typical sequence shown in figure 10.

The comparison among the three rupture-proximity curves must, of course, be considered only qualitatively. Stress rupture is a phenomenon that occurs after plastic flow, a condition likely to redistribute the stresses sufficiently to invalidate comparisons made on the basis of elastic-stress distribution.

The plots of the ratio of 2-hour stress-rupture value to the equivalent stress are not continued beyond the 6-inch radius in figure 12 because the stresses in the outer region of the disk are predominantly compressive, whereas stress rupture is associated with tensile stresses.

Stresses in rim of disk. - Plots of the ratio of elastic limit to equivalent stress are extended, in figure 12, to the outside of the disk. The temperatures and stresses corresponding to the cooled face and central plane of the disk result in plastic flow for a considerable portion of the rim. In the disk investigated, in which the rim is rendered discontinuous by the machined fir-tree slots, such plastic flow is not serious. When the disk returns to room temperature, the slots merely separate by an amount corresponding to the plastic flow, which, in the present case, is computed to be less than 0.002 inch. Loosening of the blades has, in fact, been observed in practice. The indication would seem to be that for disks of the fir-tree blade-insertion type a cold clearance between the blade and the disk is desirable in order to limit the amount of plastic flow and that close fits are unnecessary because they may precipitate plastic flow and become loose anyway; furthermore, they may increase the machining and assembly costs.

In disks of welded-blade construction, which have effectively continuous rims, the plastic flow produces residual internal strains that result in residual tensile stresses when the disk returns to room temperature. The residual stresses in a hypothetical disk similar to the one investigated, but with welded blades, have been determined by the method of reference 3 and are shown in figures 13(a) and 13(b). As a result of the stress concentrations inherent between the blades, these residual tensile stresses may be high enough to cause cracks to be propagated between blades. Such cracks have, in fact, occurred in disks with welded blades. The reduction of the high thermal stresses at the rim may be a means of preventing these cracks. As shown in figure 12, the equivalent stress exceeds the elastic limit in only a small region near the rim when the temperature distribution is that corresponding to the uncooled face of the disk, and the residual stresses (figs. 13(a) and 13(b)) are much lower than those for each of the other two temperature distributions. The higher temperature and lower gradients characteristic of the temperature distribution on the uncooled face of the disk would appear to be more desirable in disks of welded-blade construction because the equivalent stress is reduced in the rim region and the strength-to-stress ratio is increased at all points in the disk.

SUMMARY OF RESULTS

An experimental investigation was conducted to determine the temperature distribution in an aircraft-engine gas-turbine disk. The stresses in the turbine disk were calculated from the measured temperature distribution.

The maximum radial temperature gradient was 1050° F on the cooled face of the disk. A temperature gradient as high as 600° F existed between the two faces of the disk near the axis of rotation; the upstream face was air cooled, the downstream face was uncooled. Stresses introduced by the axial temperature gradients were neglected in the calculations.

By use of the temperature distribution in the central plane to determine the gross behavior of the disk, the stresses in the inner region were found to be at all times lower than the proportional elastic limit and very much lower than the 2-hour stress-rupture value.

By use of the temperature distribution in the cooled face as representative of the temperature distribution that would exist throughout the thickness of the disk if both faces were cooled, and by use of the temperature distribution on the uncooled face as representative of the temperature distribution that would exist throughout the thickness of the disk if no cooling air were passed over either face, it was found that removing the cooling air would increase the strength-to-stress ratio at all points in the disk.

The lower temperature gradients characteristic of the temperature distribution on the uncooled face of the disk also appeared to be more desirable in disks of welded-blade construction because the equivalent stress was reduced in the rim region and strength-to-stress ratio was increased at all points in the disk.

The emergency take-off sequence results in stress states differing only slightly from those present during the typical take-off sequence.

Flight Propulsion Research Laboratory,
National Advisory Committee for Aeronautics,
Cleveland, Ohio.

REFERENCES

1. Farmer, J. Elmo: Relation of Nozzle-Blade and Turbine-Bucket Temperatures to Gas Temperatures in a Turbojet Engine. NACA RM No. E7L12, 1948.

2. Manson, S. S.: The Determination of the Elastic Stresses in Gas-Turbine Disks. NACA TN No. 1279, 1947.

3. Millenson, M. B., and Manson, S. S.: Determination of Stresses in Gas-Turbine Disks Subjected to Plastic Flow and Creep. NACA TN No. 1636, 1948.

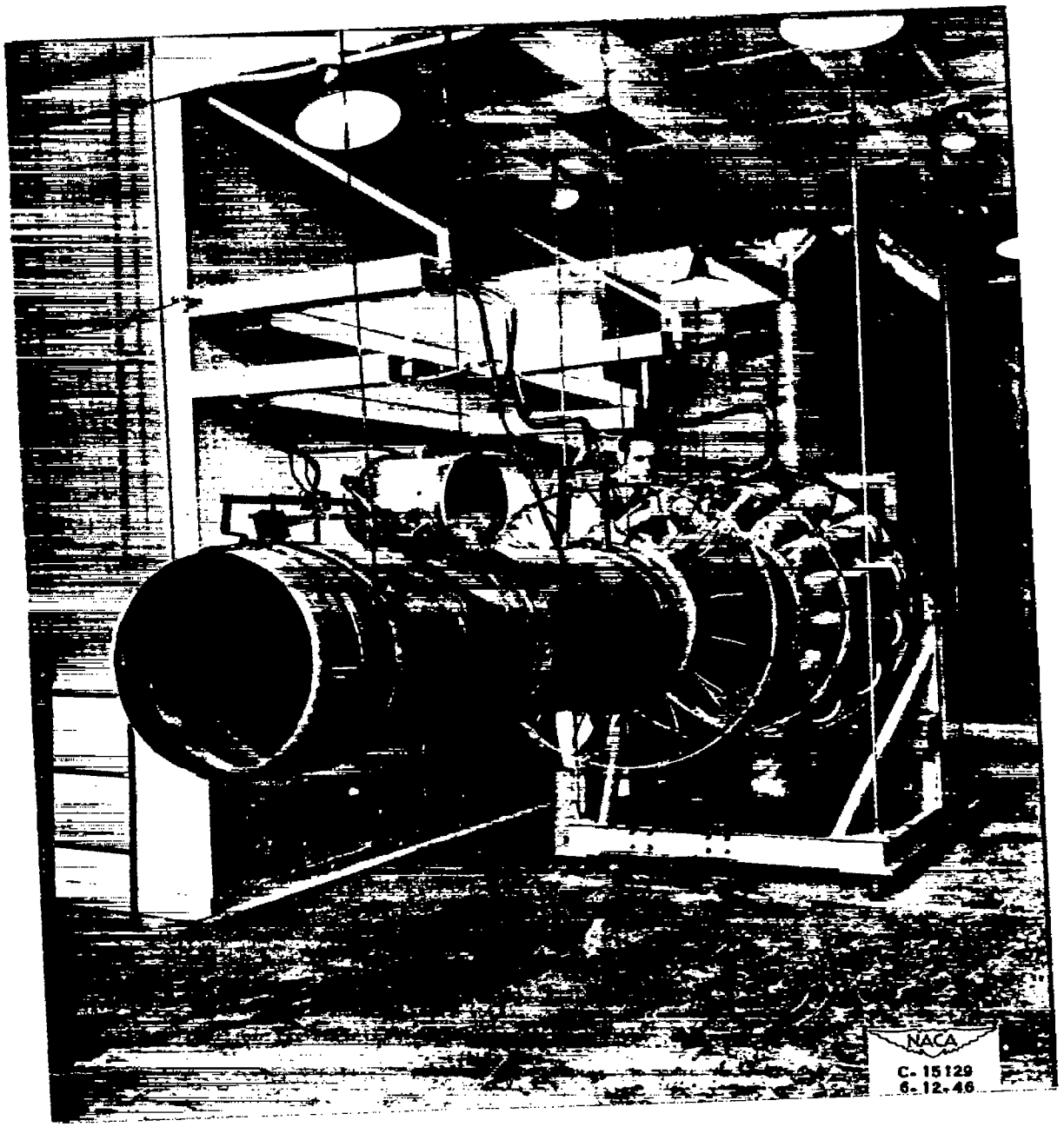

Figure 1. - Turbojet engine mounted on pendulum-type sea-level test stand showing NACA variable-area jet nozzle used to control gas temperature in exhaust cone.

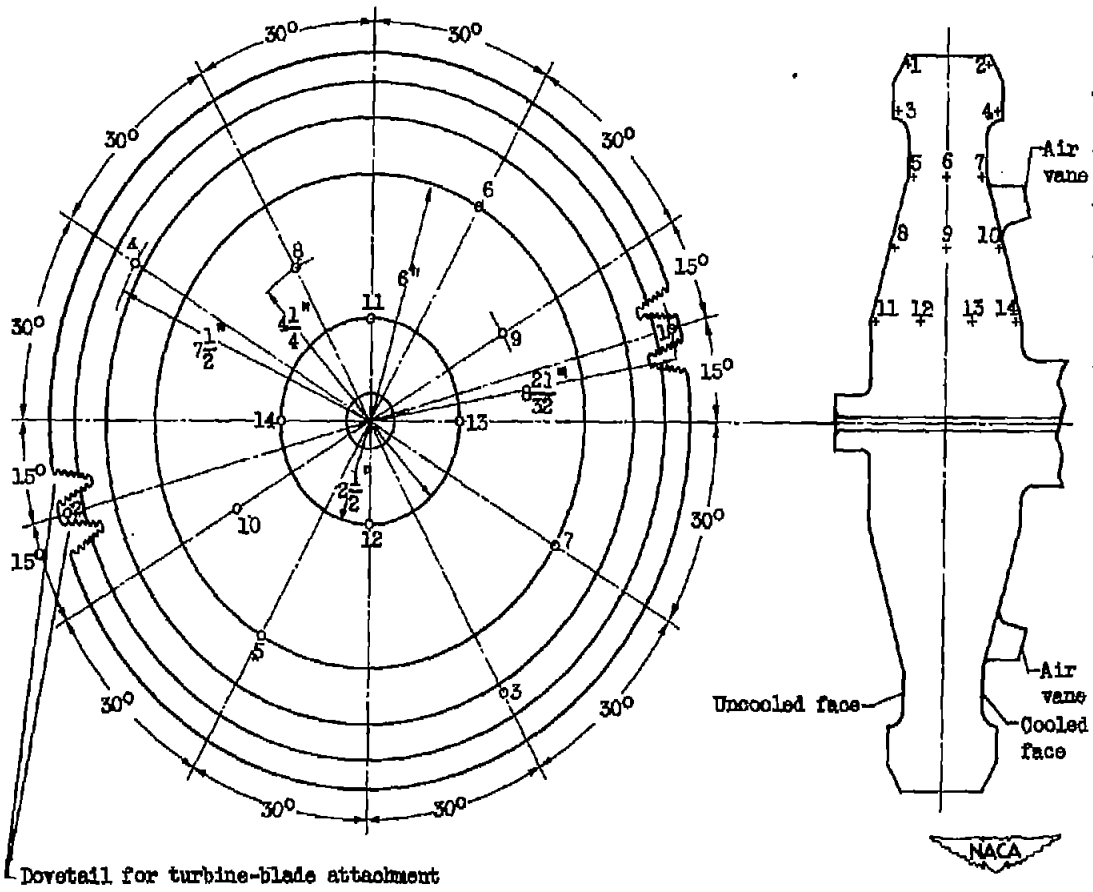

Thermocouple	Distance (in.)	
	From cooled face	From uncooled face
1		1/8
2	1/8	
3		1/8
4	1/8	
5		1/8
6		1 3/16
7	1/8	
8		1/8
9		1 11/16
10	1/8	
11		1/8
12		1 7/8
13	1 7/8	
14	1/8	

Figure 2. - Location of thermocouples on turbine disk.

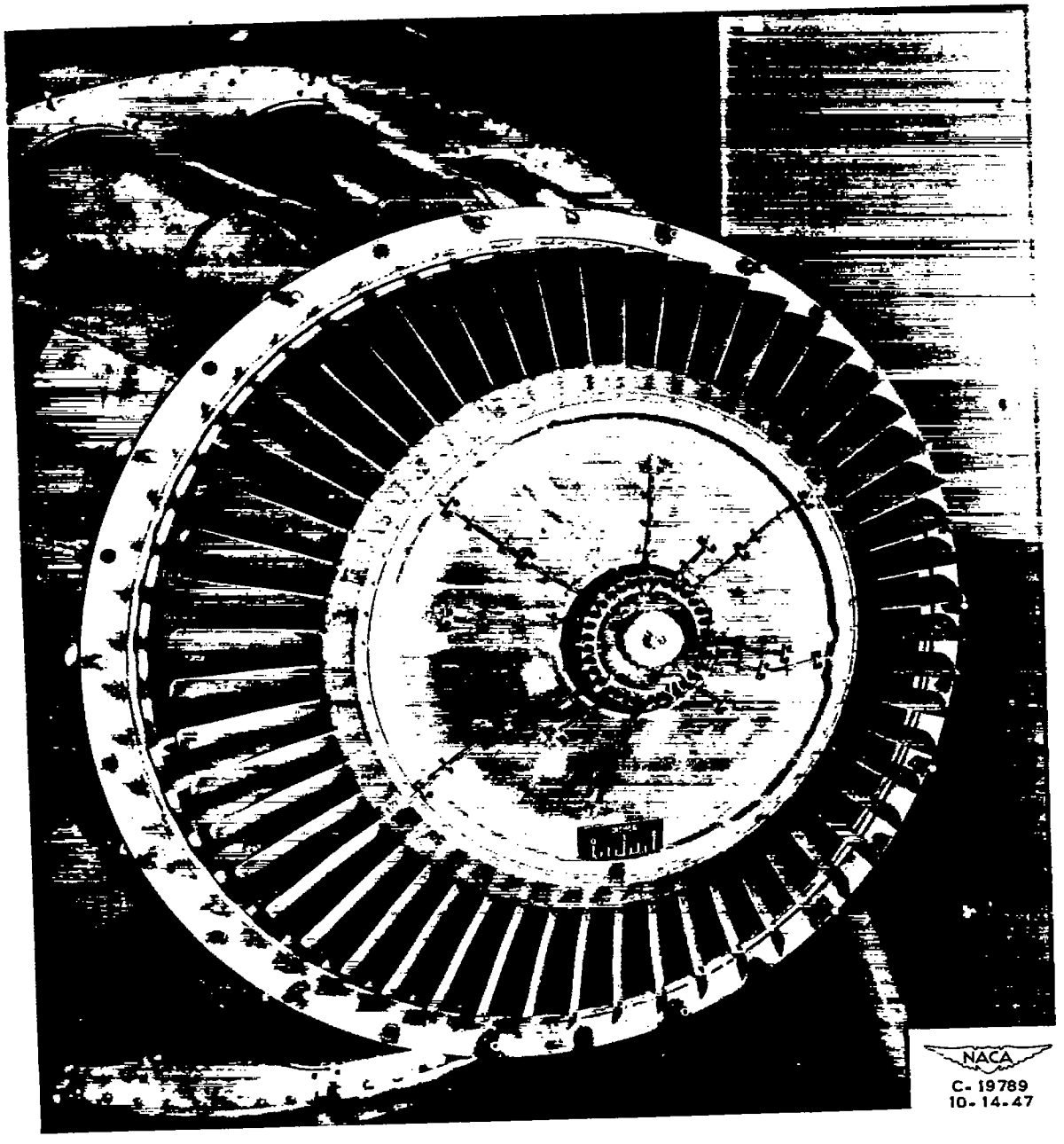

Figure 3. - Method of installing thermocouples on turbine disk.

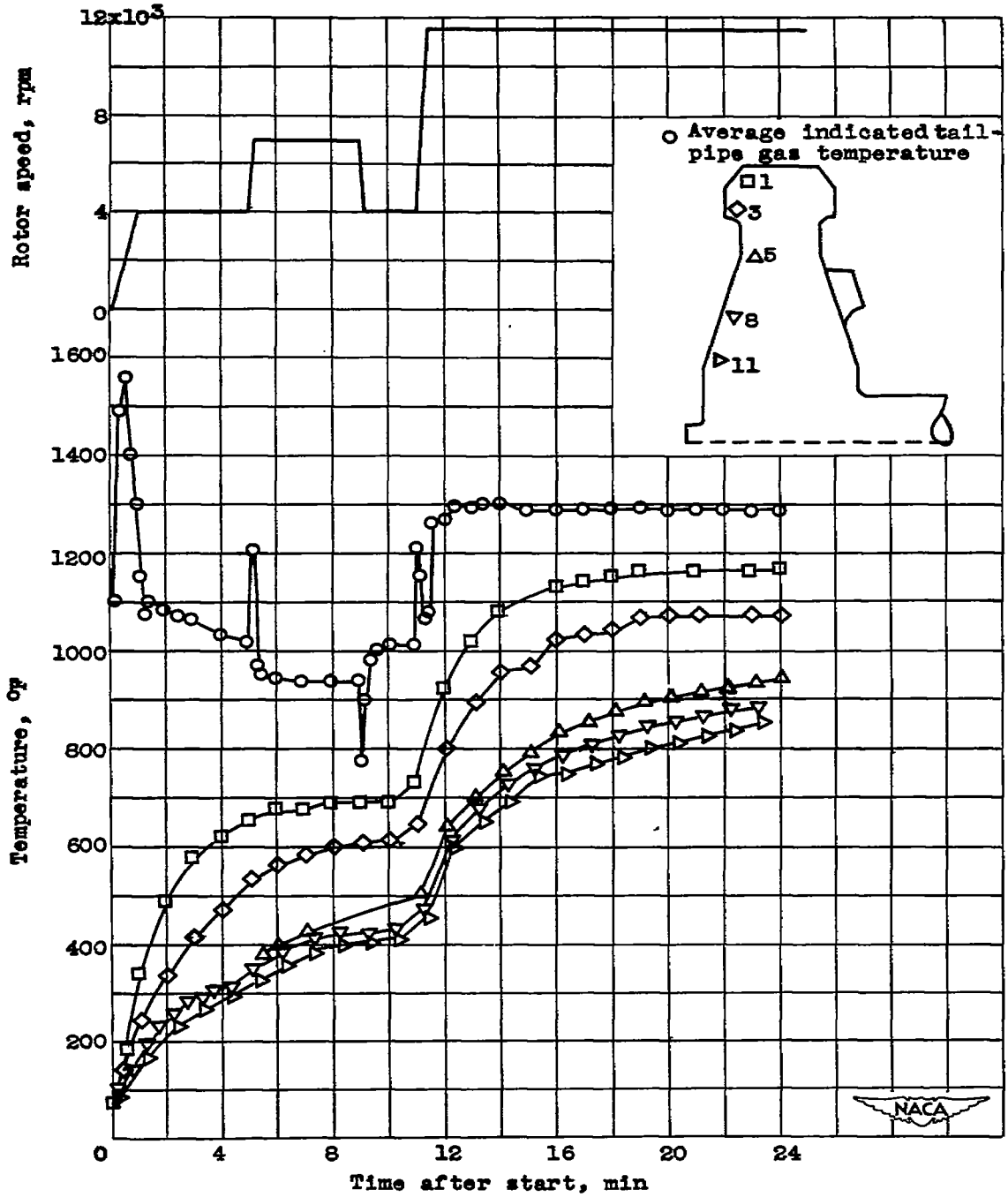

(a) Uncooled face of turbine disk.

Figure 4. - Variation of turbine-disk temperature with time during typical take-off sequence.

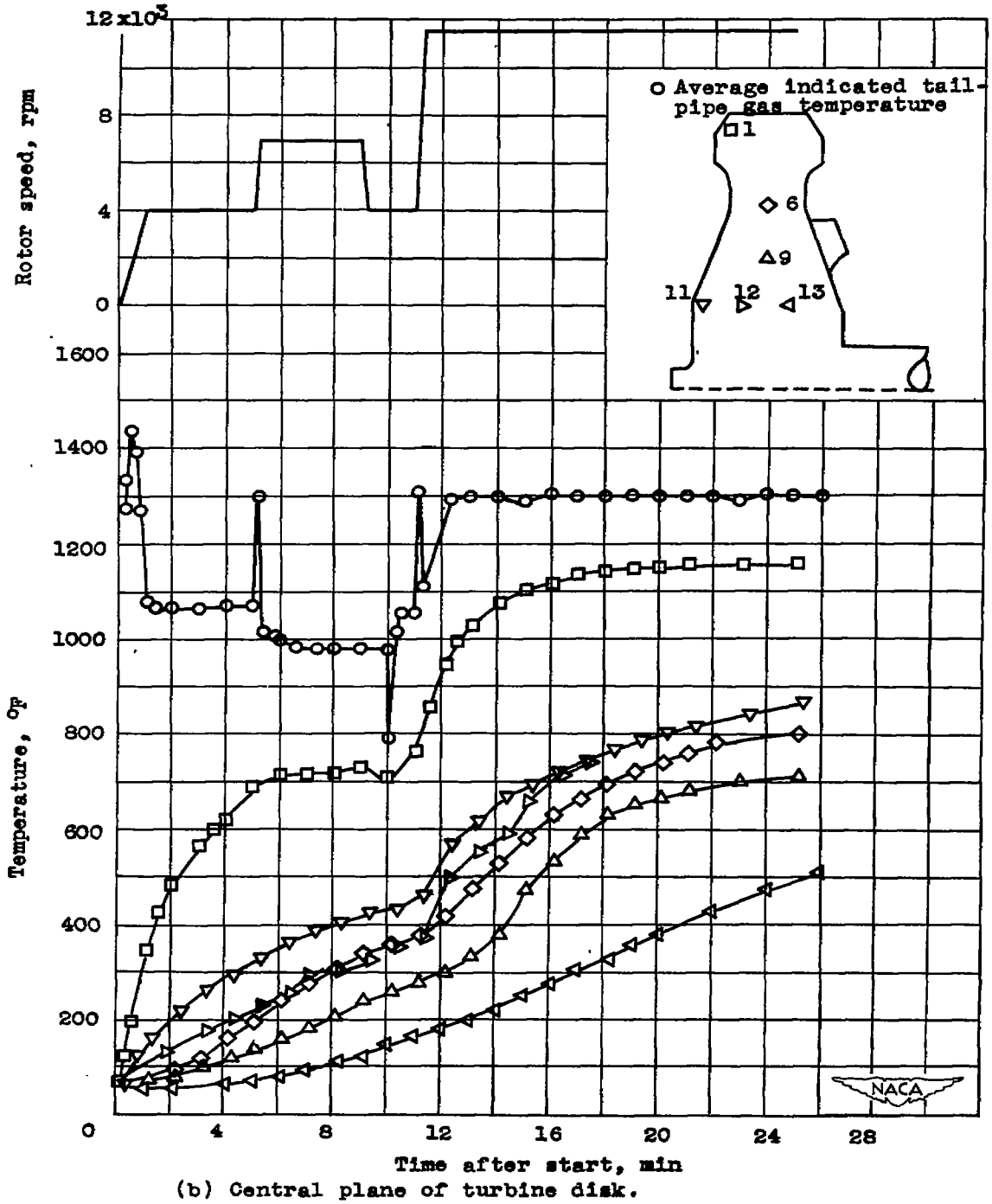

(b) Central plane of turbine disk.

Figure 4. - Continued. Variation of turbine-disk temperature with time during typical take-off sequence.

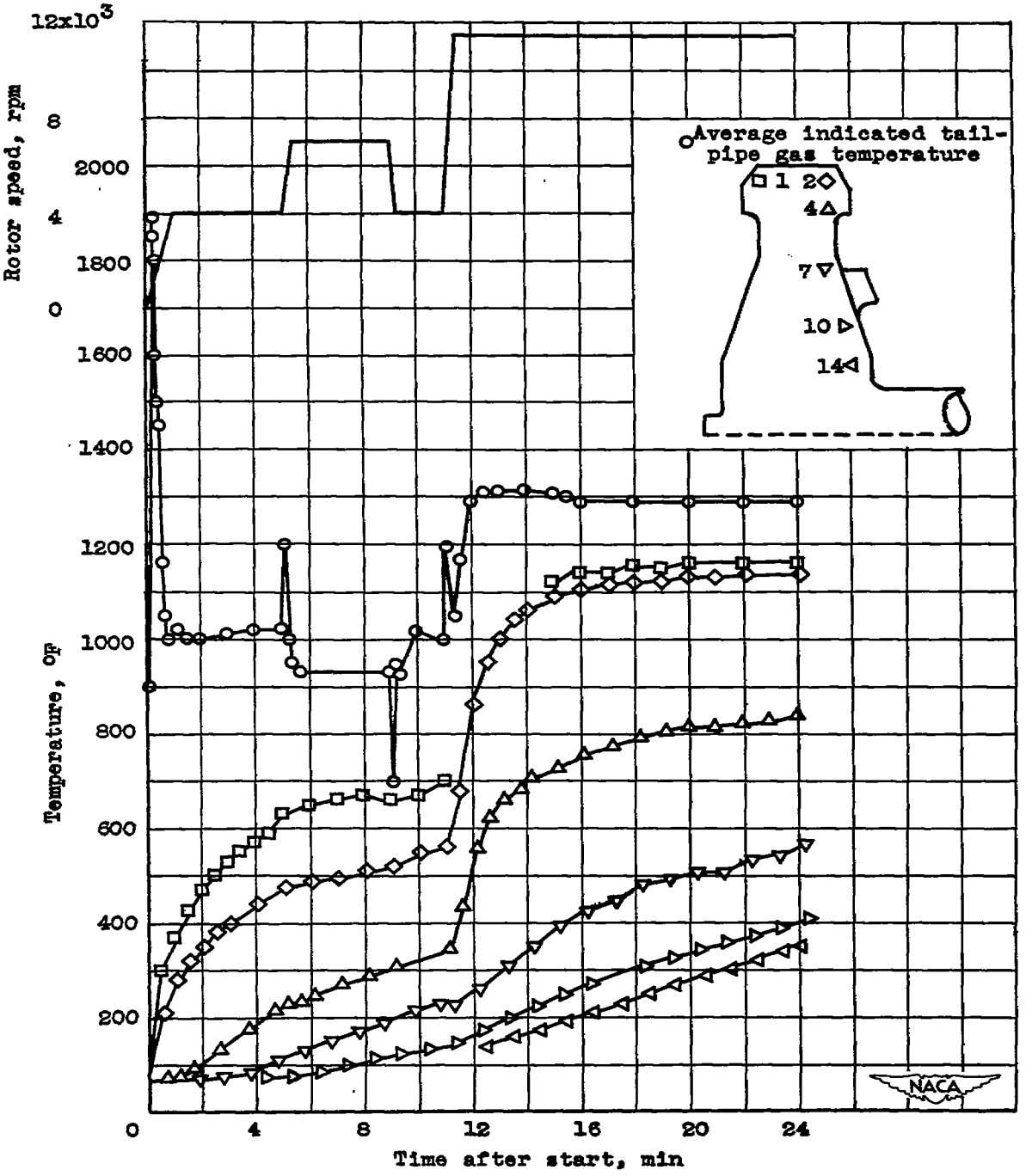

(c) Cooled face of turbine disk.

Figure 4. - Concluded. Variation of turbine-disk temperature with time during typical take-off sequence.

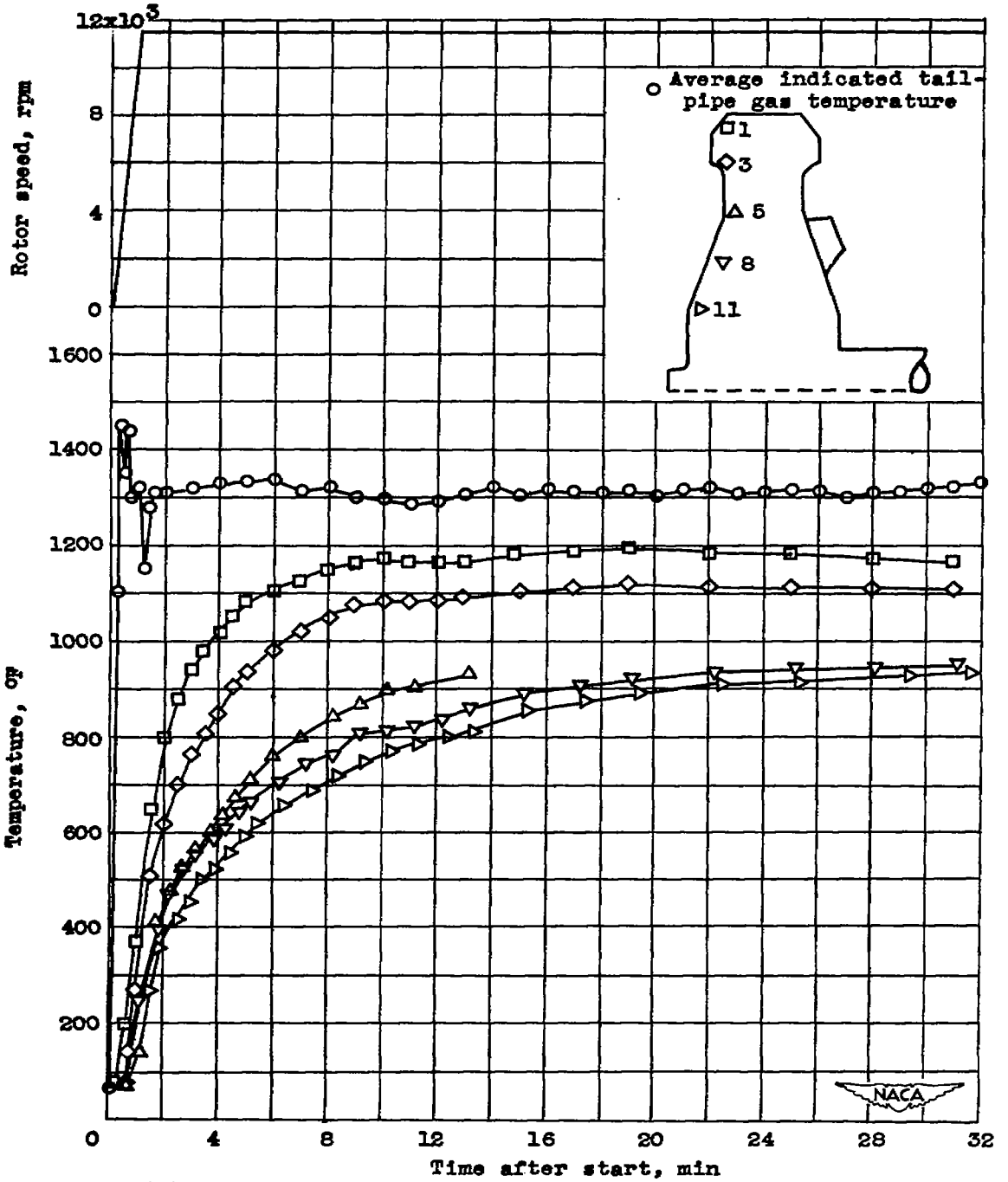

(a) Uncooled face of turbine disk.

Figure 5. - Variation of turbine-disk temperature with time during emergency take-off sequence.

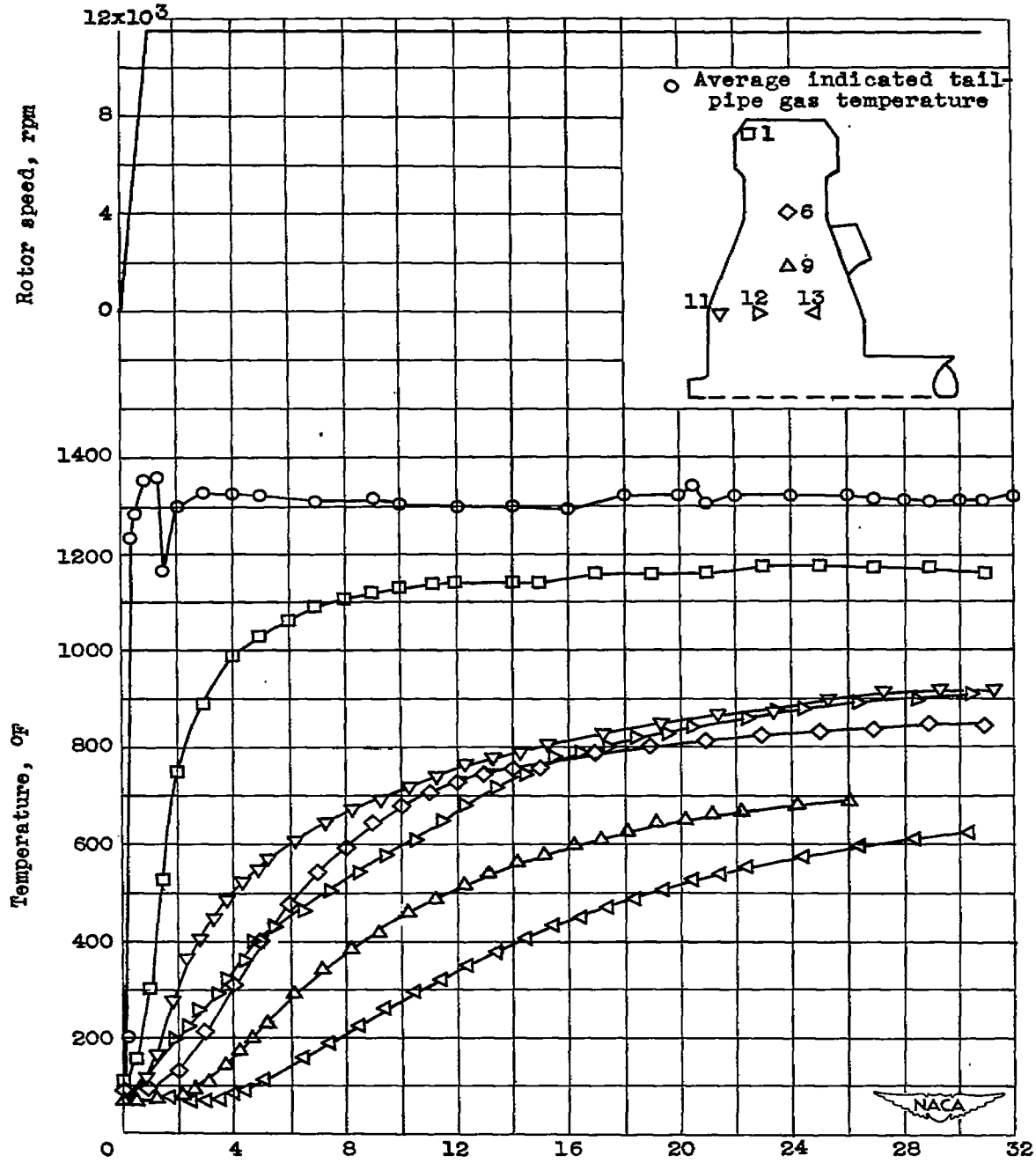

(b) Central plane of turbine disk.

Figure 5. - Continued. Variation of turbine-disk temperature with time during emergency take-off sequence.

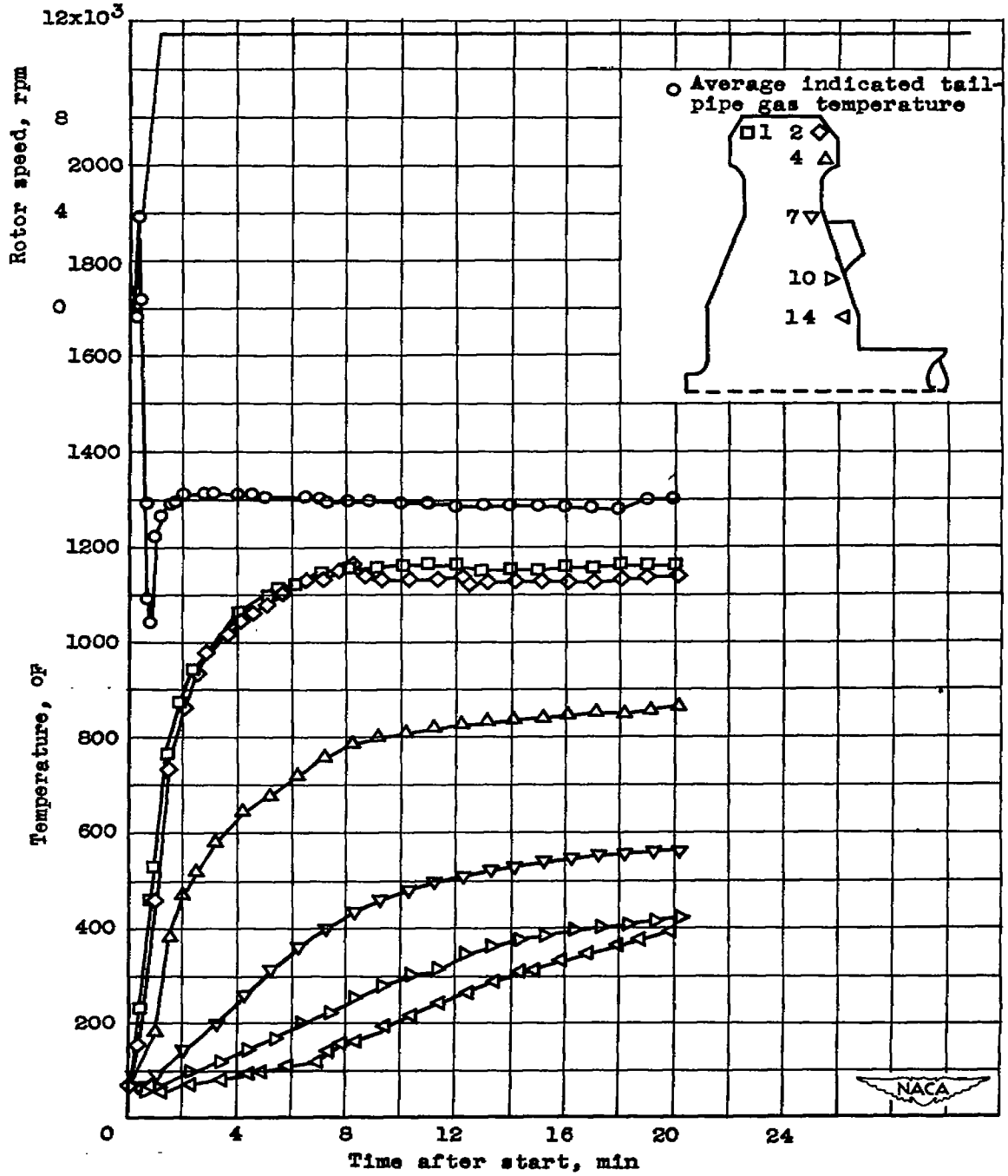

(c) Cooled face of turbine disk.

Figure 5. - Concluded. Variation of turbine-disk temperature with time during emergency take-off sequence.

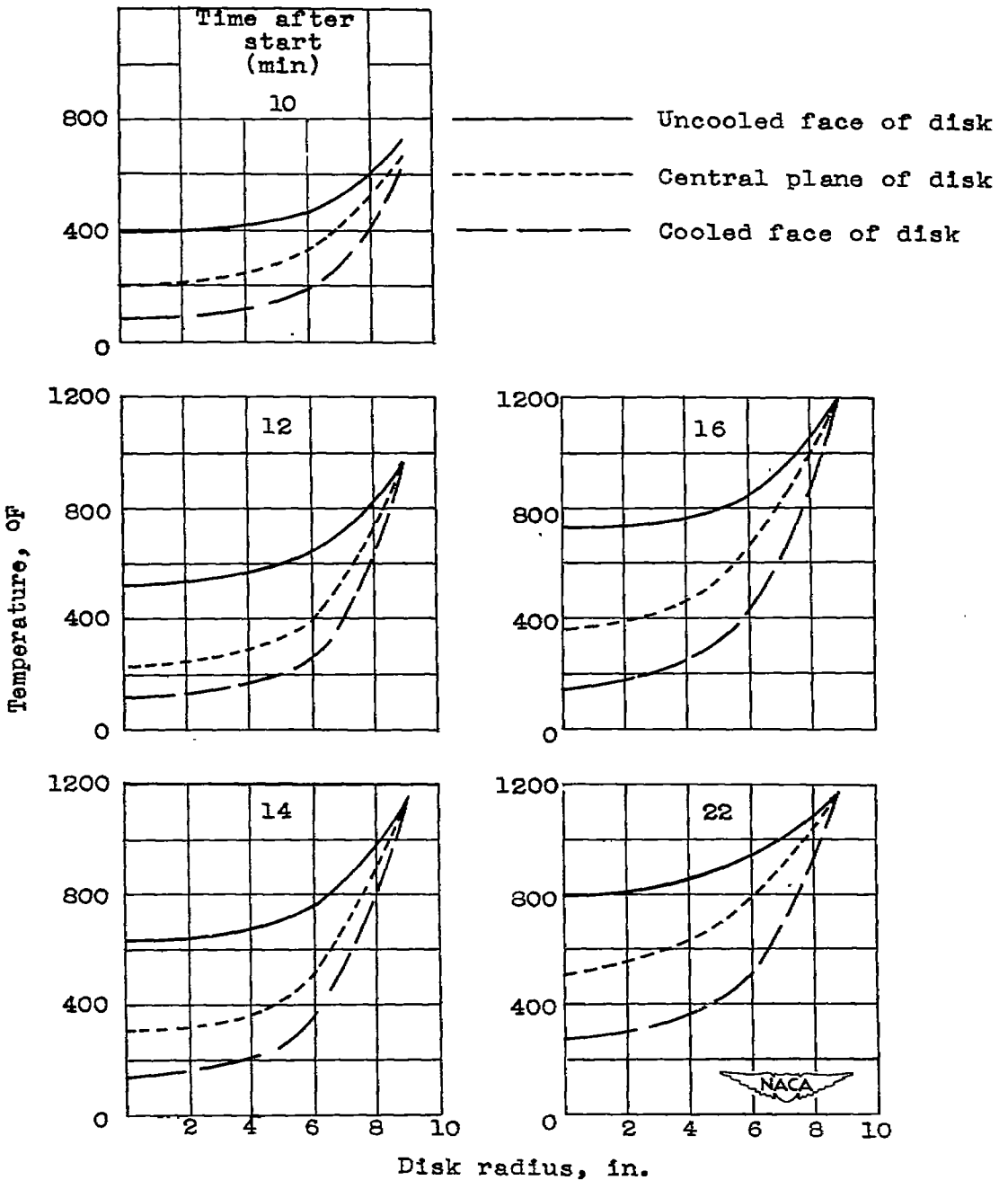

(a) Typical take-off sequence.

Figure 6. - Radial temperature distributions on cooled and uncooled faces and central plane of turbine disk at various times after starting.

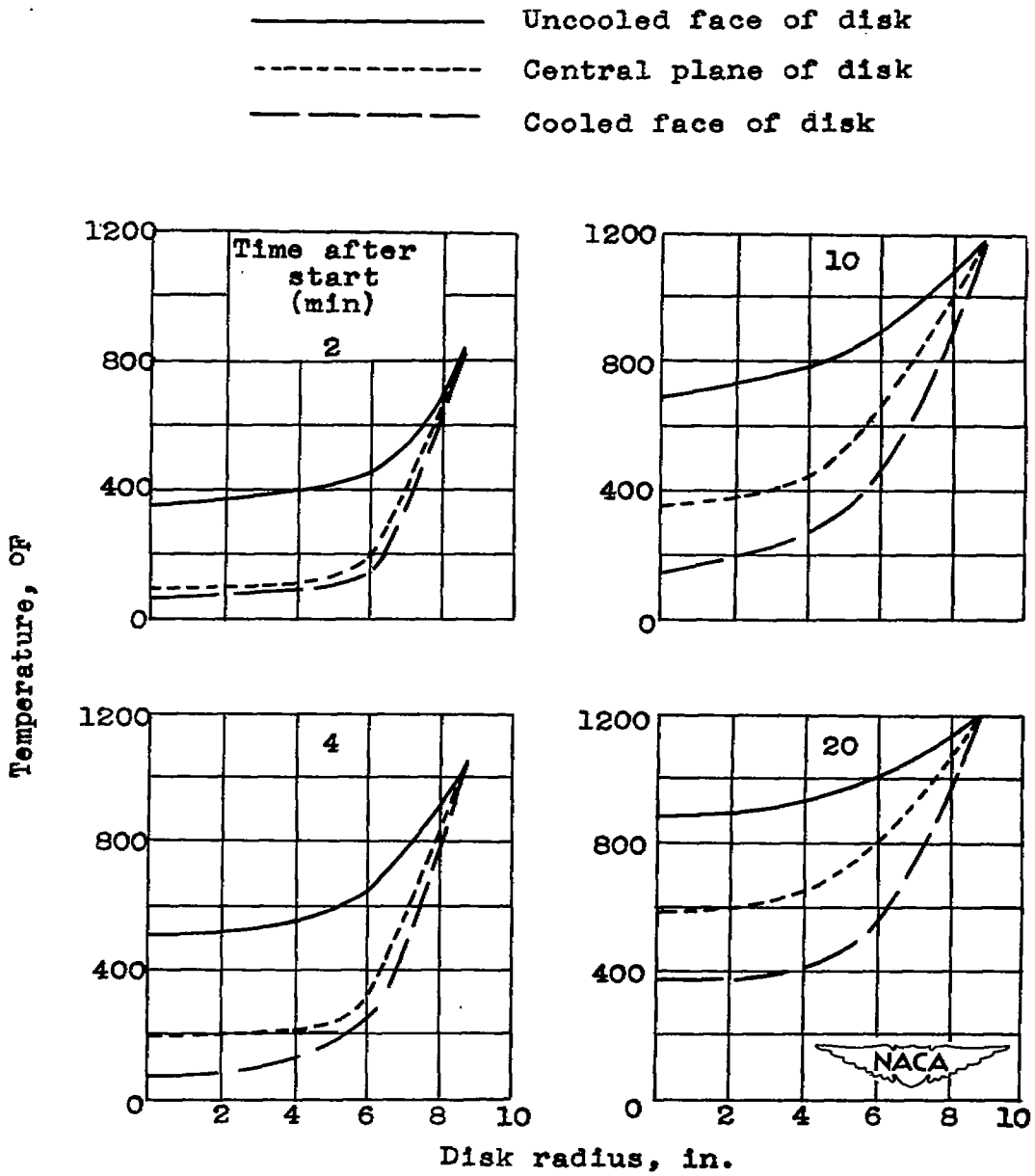

(b) Emergency take-off sequence.

Figure 6. - Concluded. Radial temperature distributions on cooled and uncooled faces and central plane of turbine disk at various times after starting.

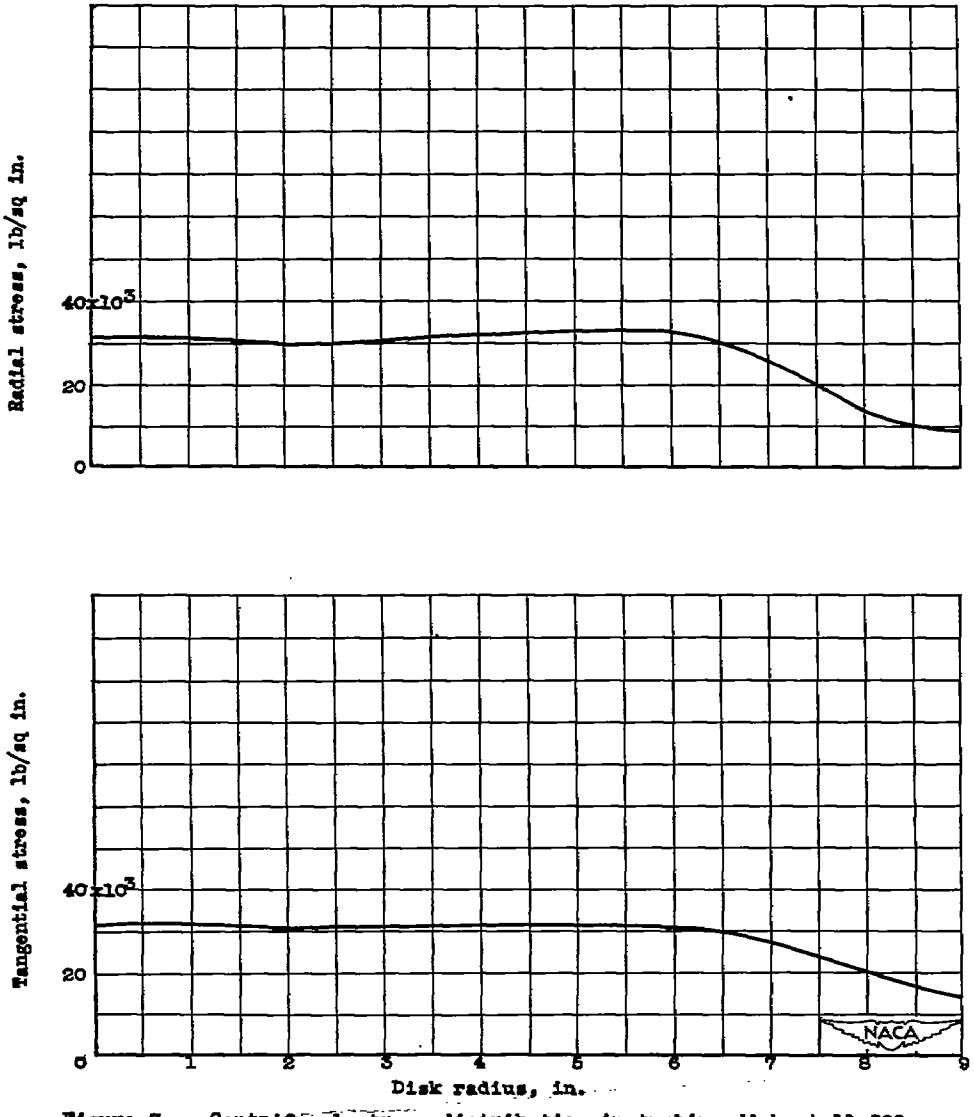

Figure 7. - Centrifugal stress distribution in turbine disk at 11,500 rpm, after 14 minutes of operation in typical take-off sequence.

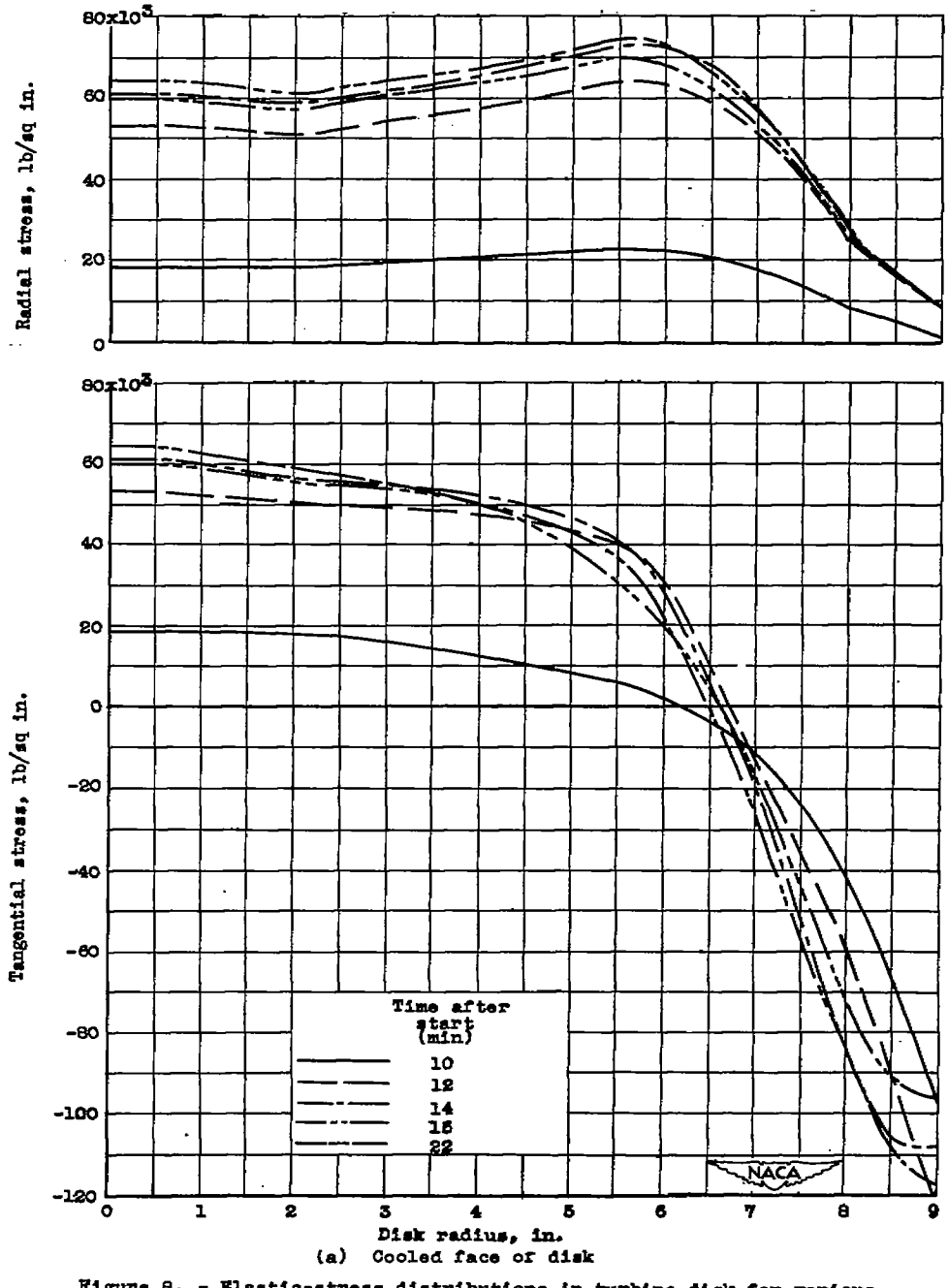

(a) Cooled face or disk

Figure 8. - Elastic-stress distributions in turbine disk for various times during typical take-off sequence.

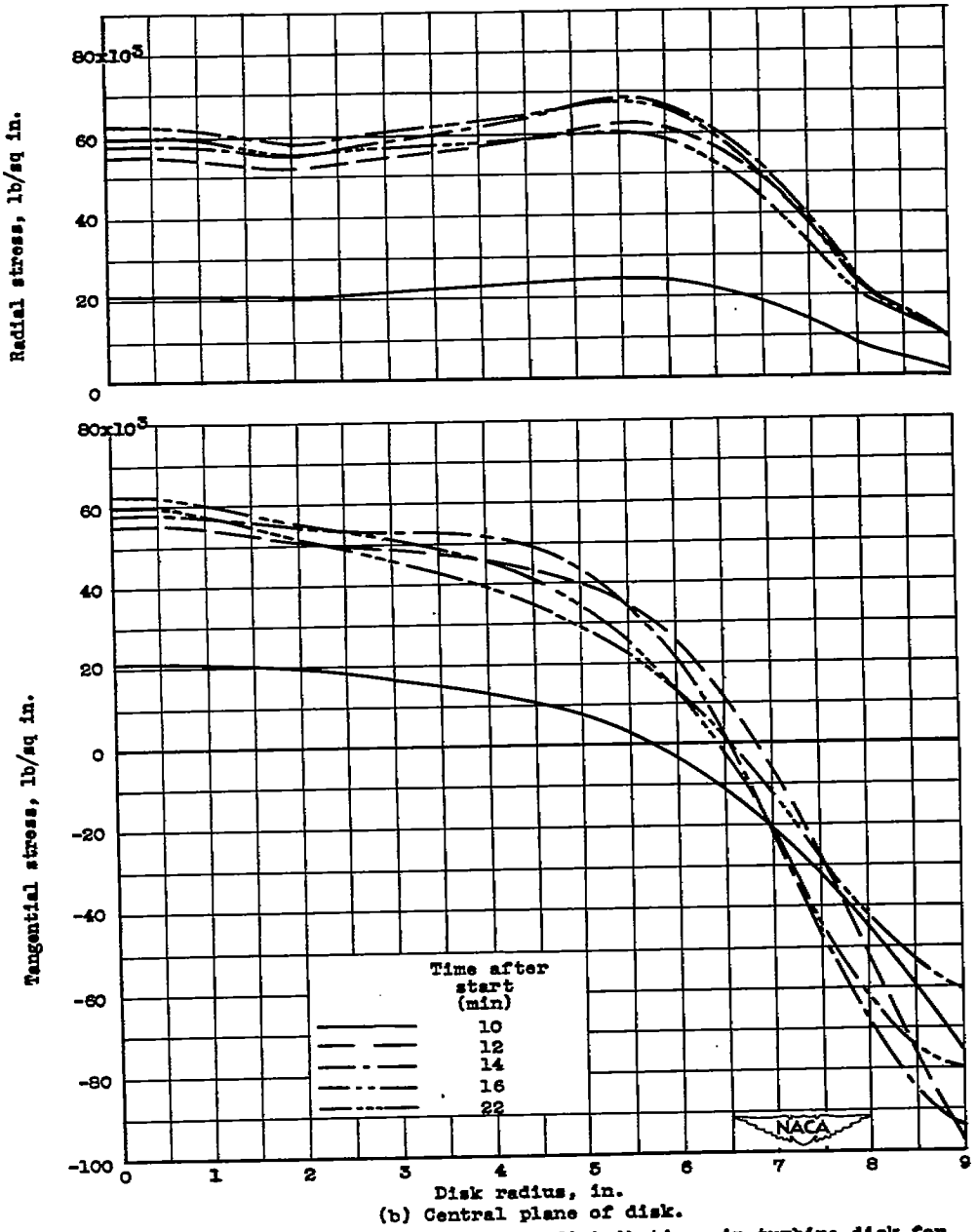

(b) Central plane of disk.

Figure 8. - Continued. Elastic-stress distributions in turbine disk for various times during typical take-off sequence.

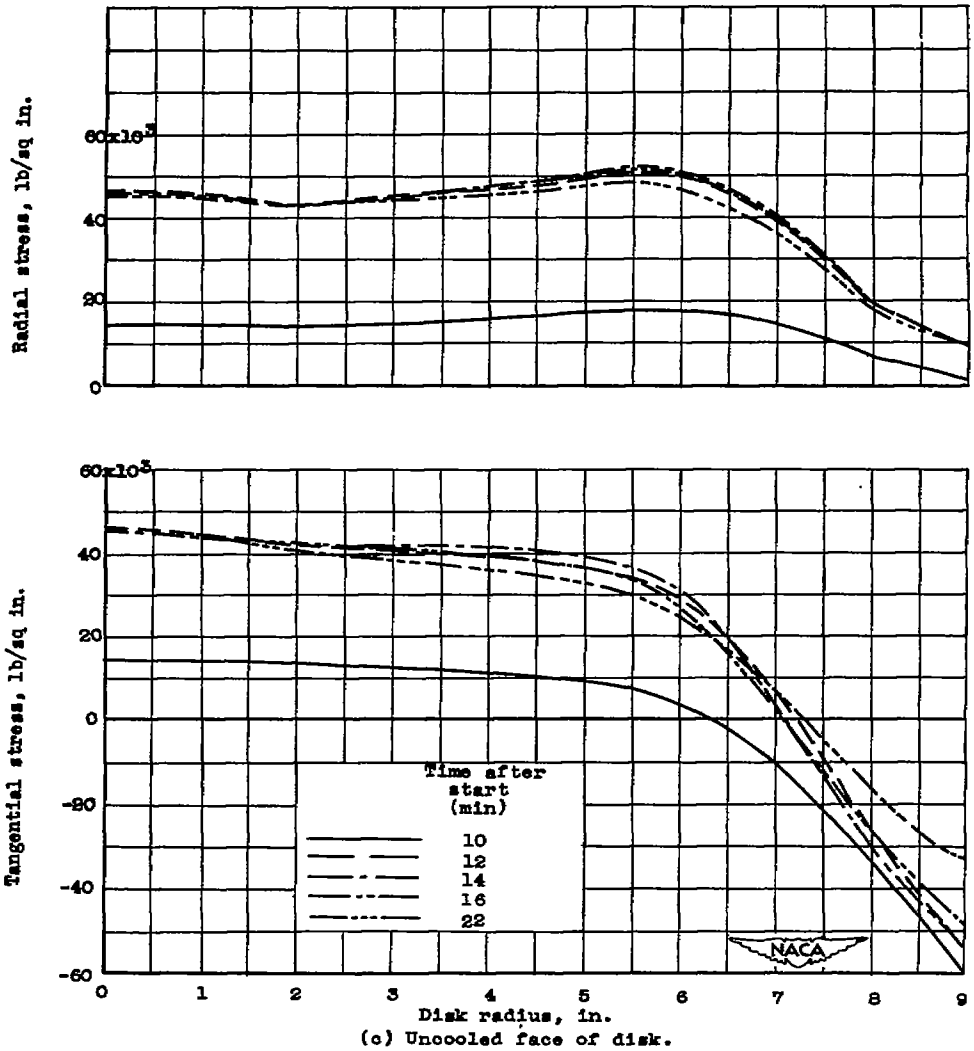

(c) Uncooled face of disk.

Figure 8. - Concluded. Elastic-stress distributions in turbine disk for various times during typical take-off sequence.

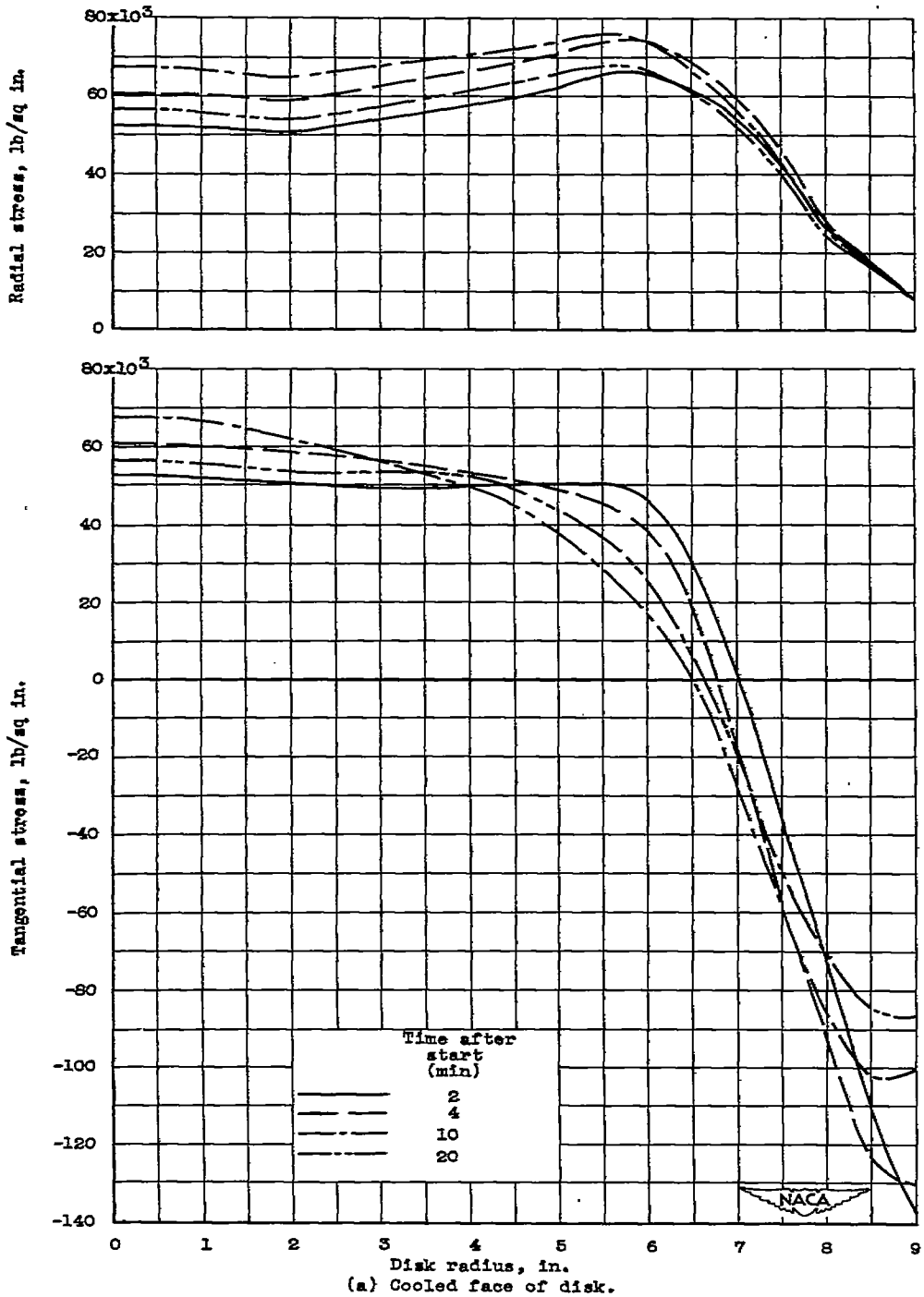

(a) Cooled face of disk.

Figure 9. - Elastic-stress distributions in turbine disk for various times during emergency take-off sequence.

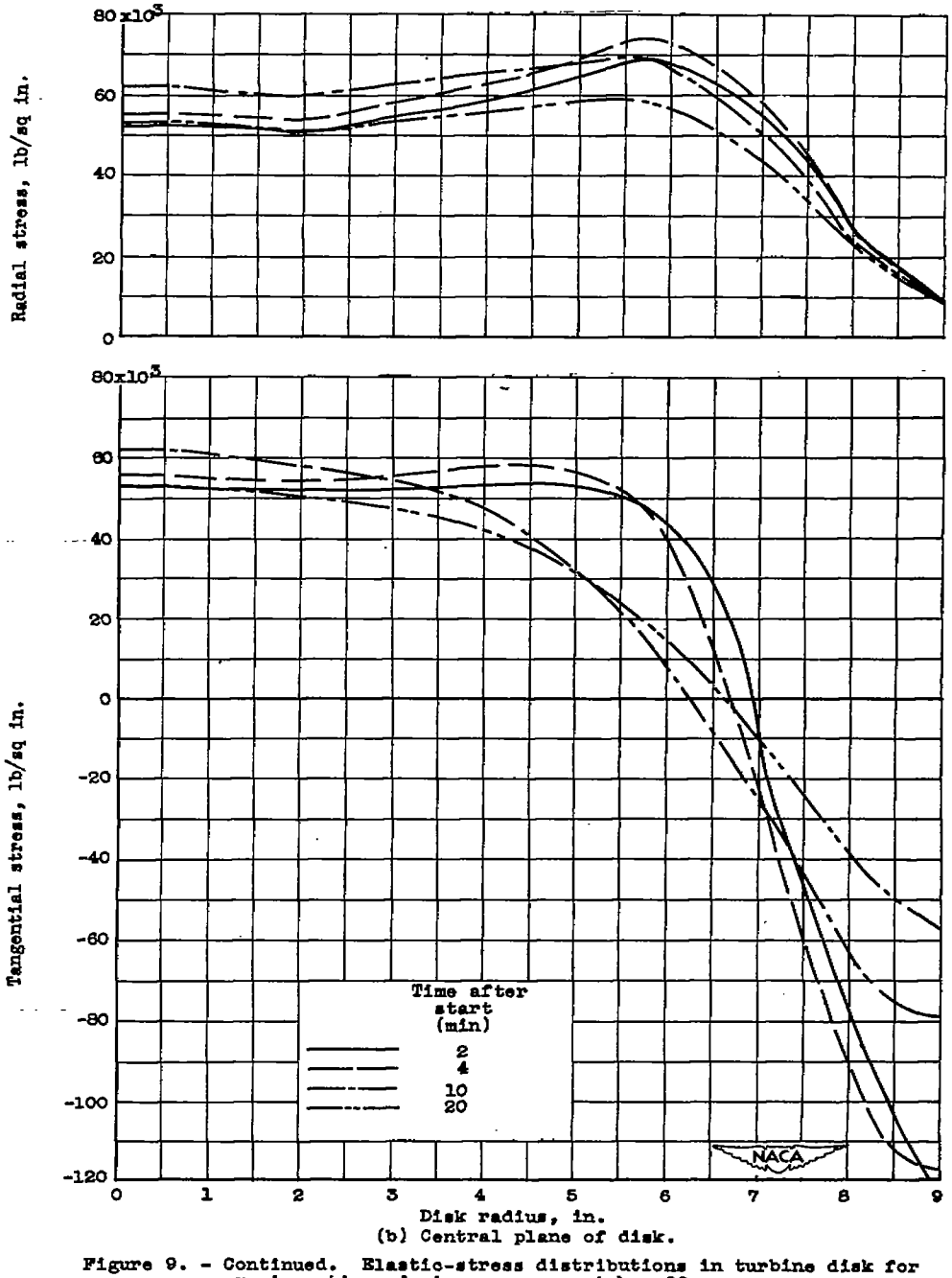

(b) Central plane of disk.

Figure 9. - Continued. Elastic-stress distributions in turbine disk for various times during emergency take-off sequence.

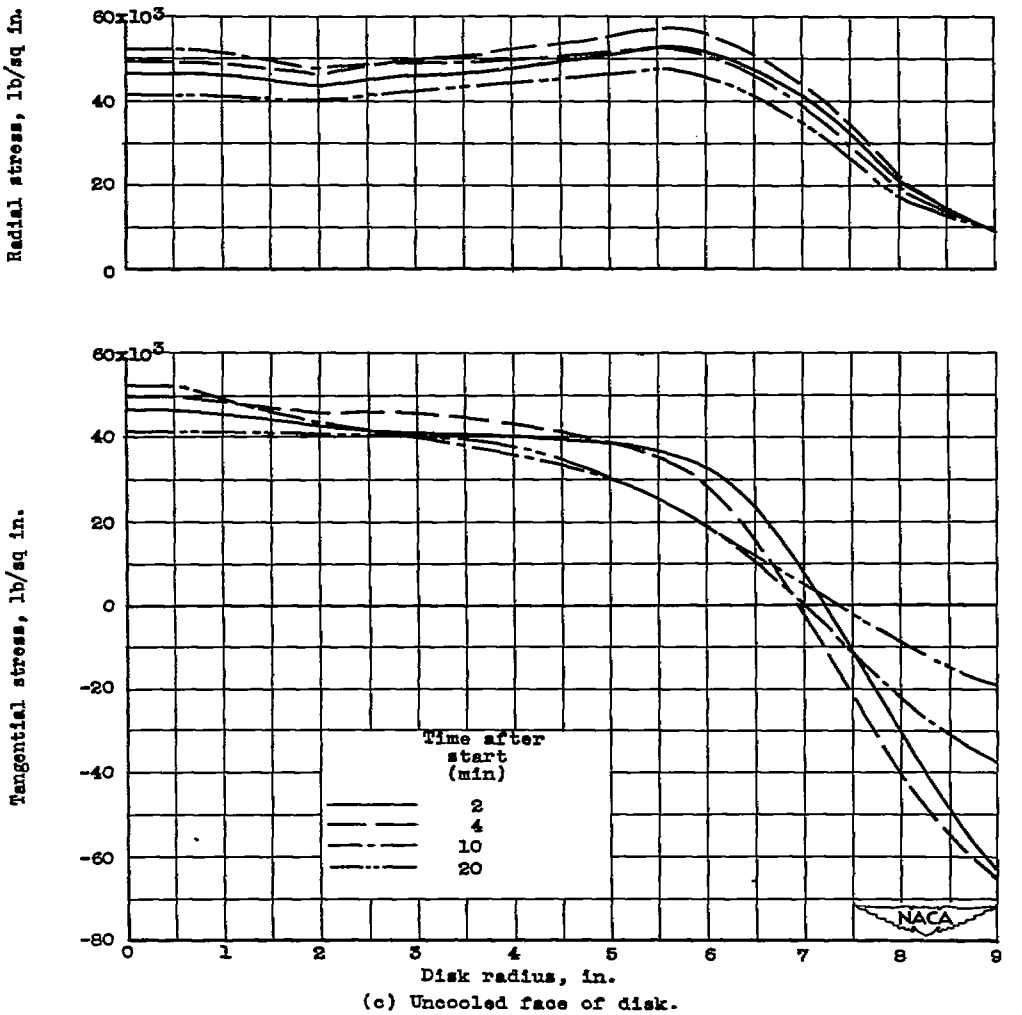

(c) Uncooled face of disk.

Figure 9. - Concluded. Elastic-stress distributions in turbine disk for various times during emergency take-off sequence.

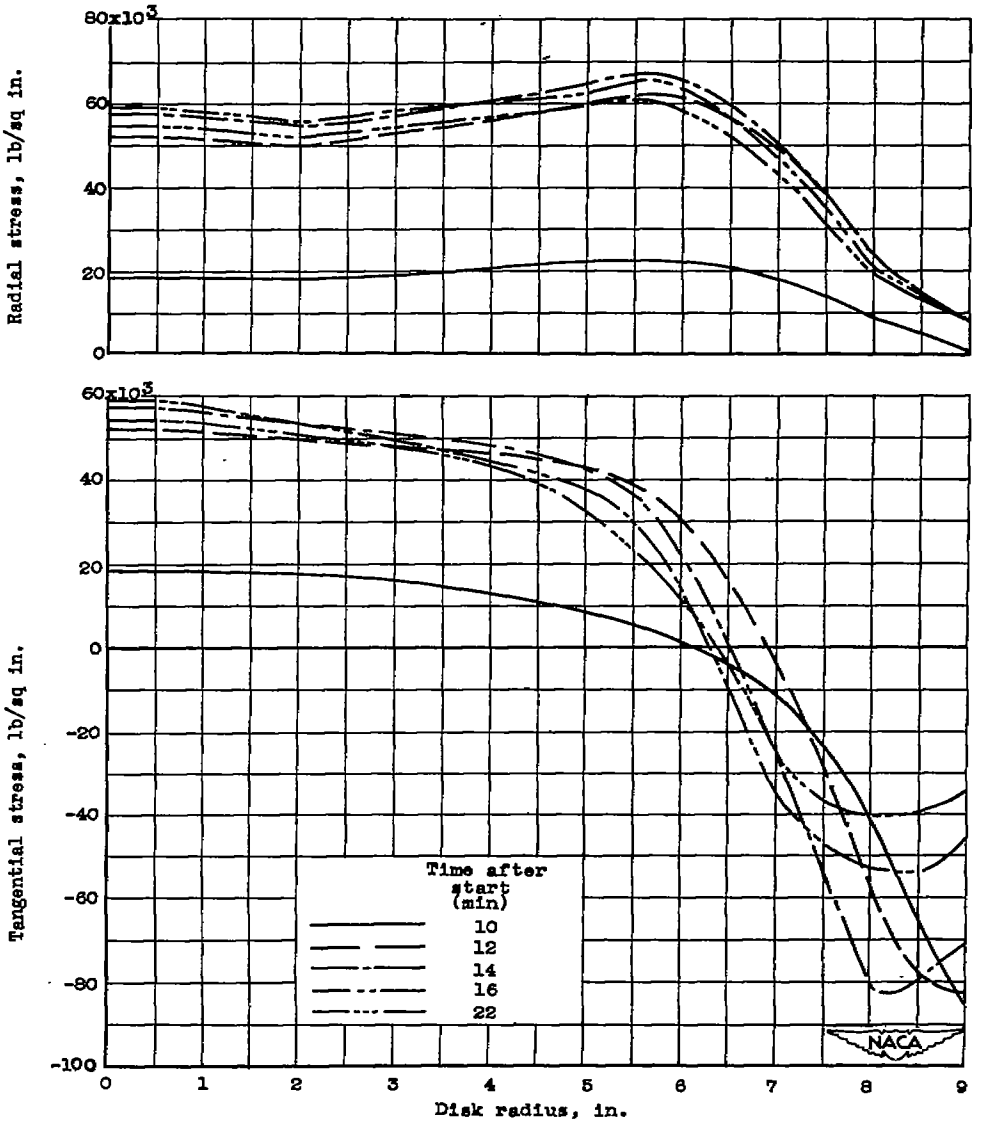

(a) Cooled face of disk.

Figure 10. - Plastic-stress distributions in turbine disk for various times during typical take-off sequence.

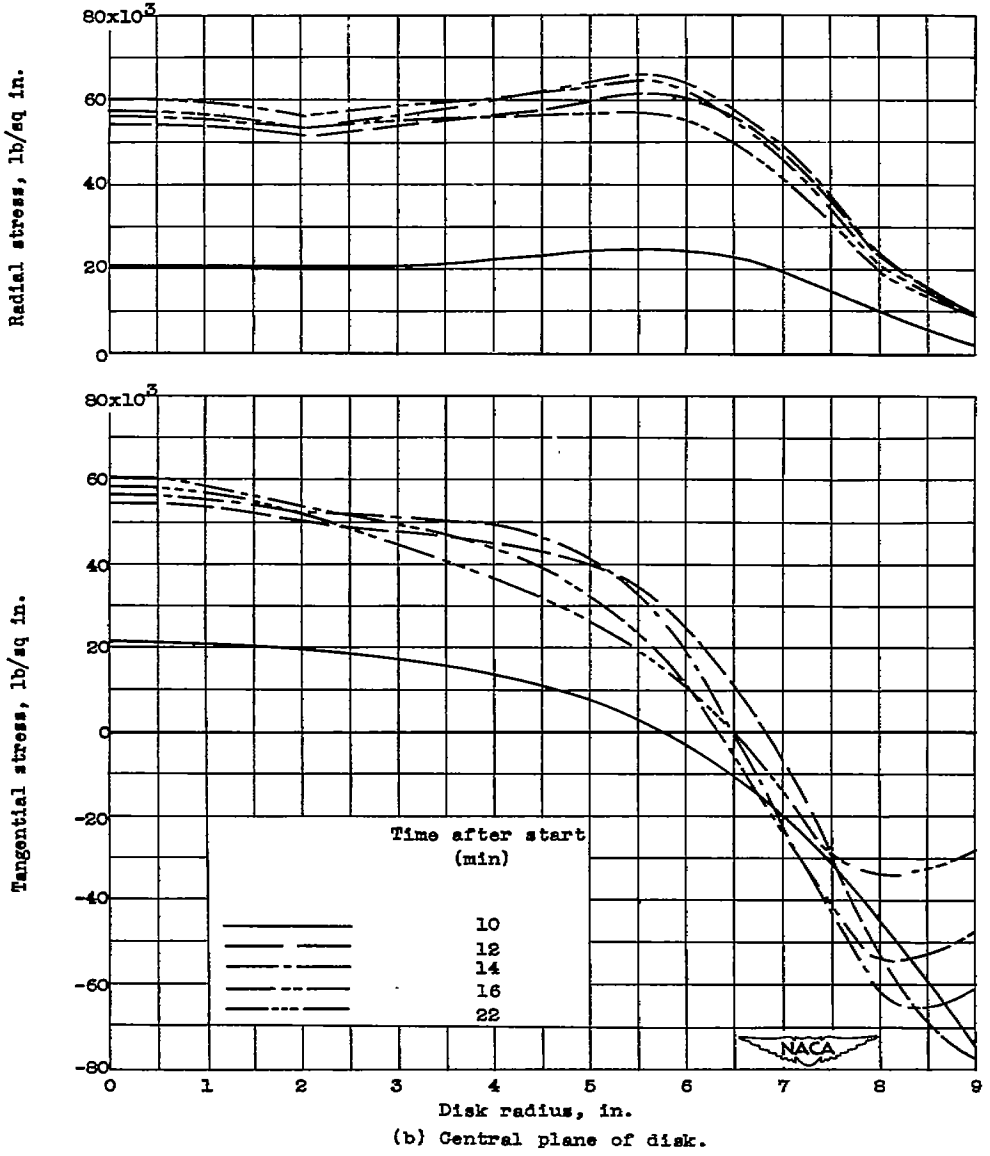

(b) Central plane of disk.

Figure 10. - Continued. Plastic-stress distributions in turbine disk for various times during typical take-off sequence.

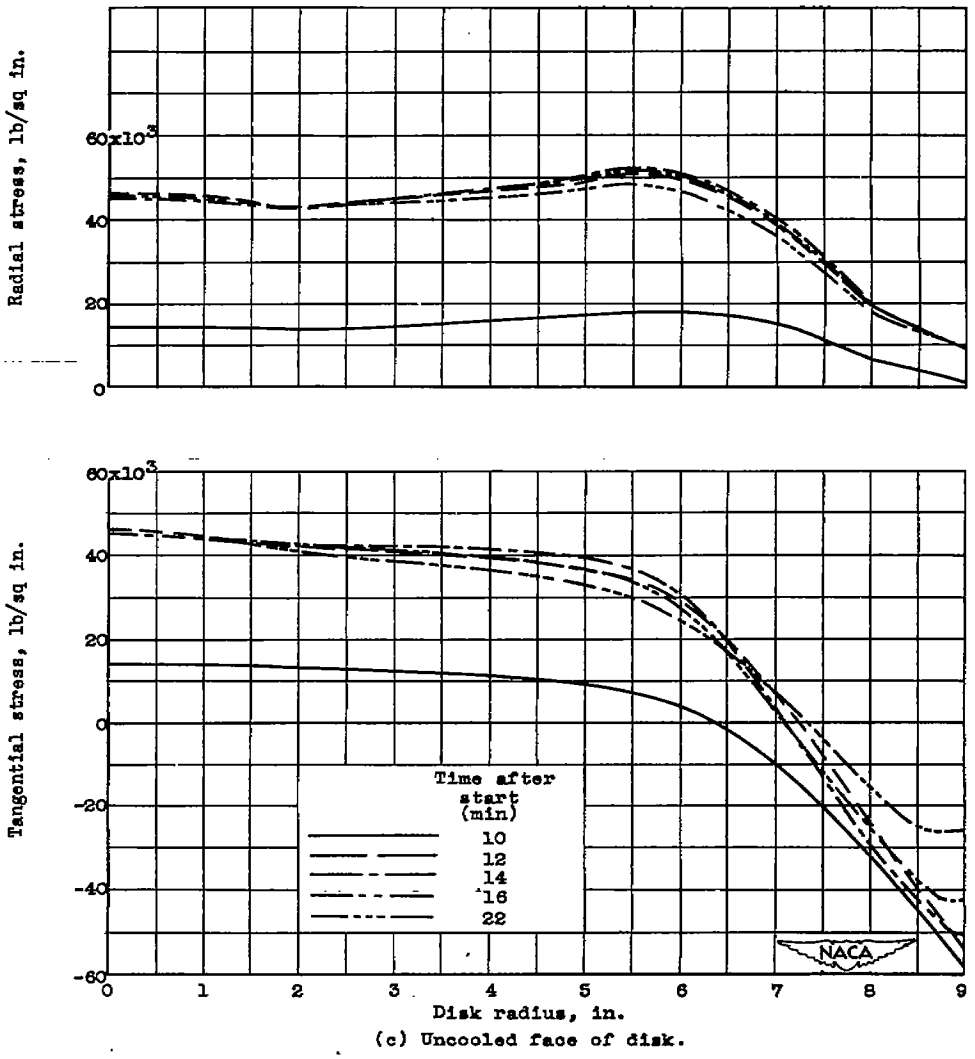

(c) Uncooled face of disk.

Figure 10. - Concluded. Plastic-stress distributions in turbine disk for various times during typical take-off sequence.

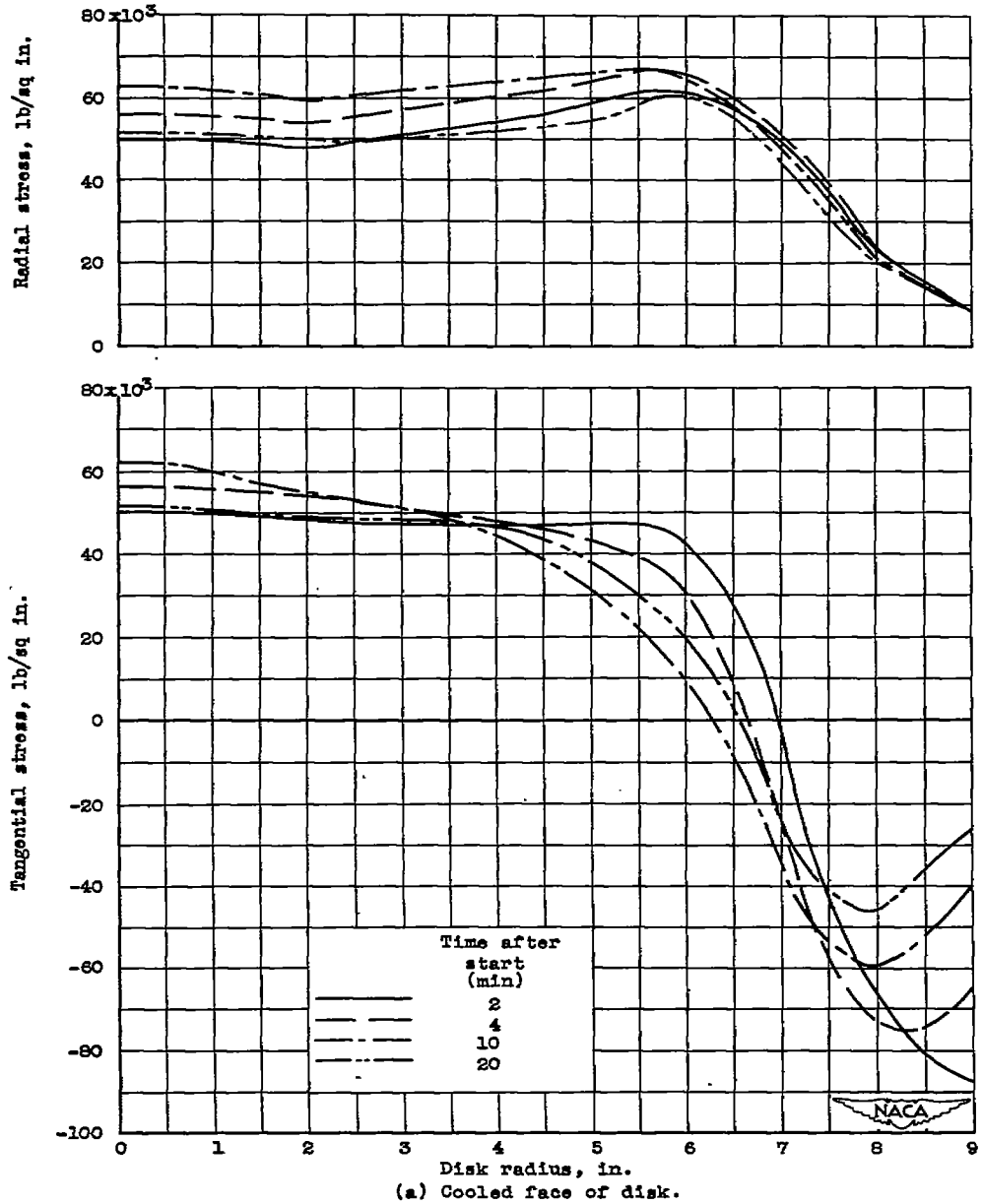

(a) Cooled face of disk.

Figure 11. - Plastic-stress distributions in turbine disk for various times during emergency take-off sequence.

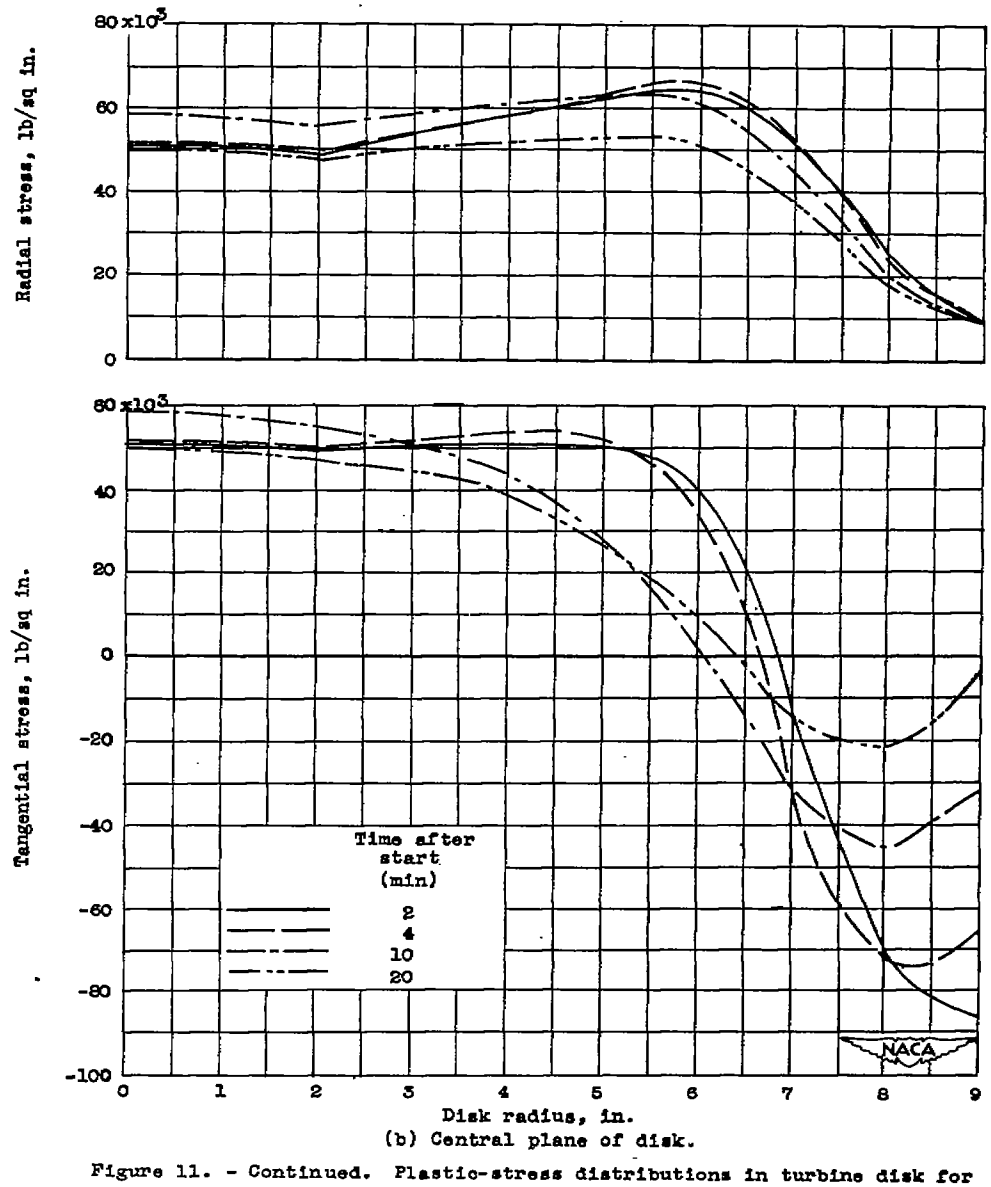

(b) Central plane of disk.

Figure 11. - Continued. Plastic-stress distributions in turbine disk for various times during emergency take-off sequence.

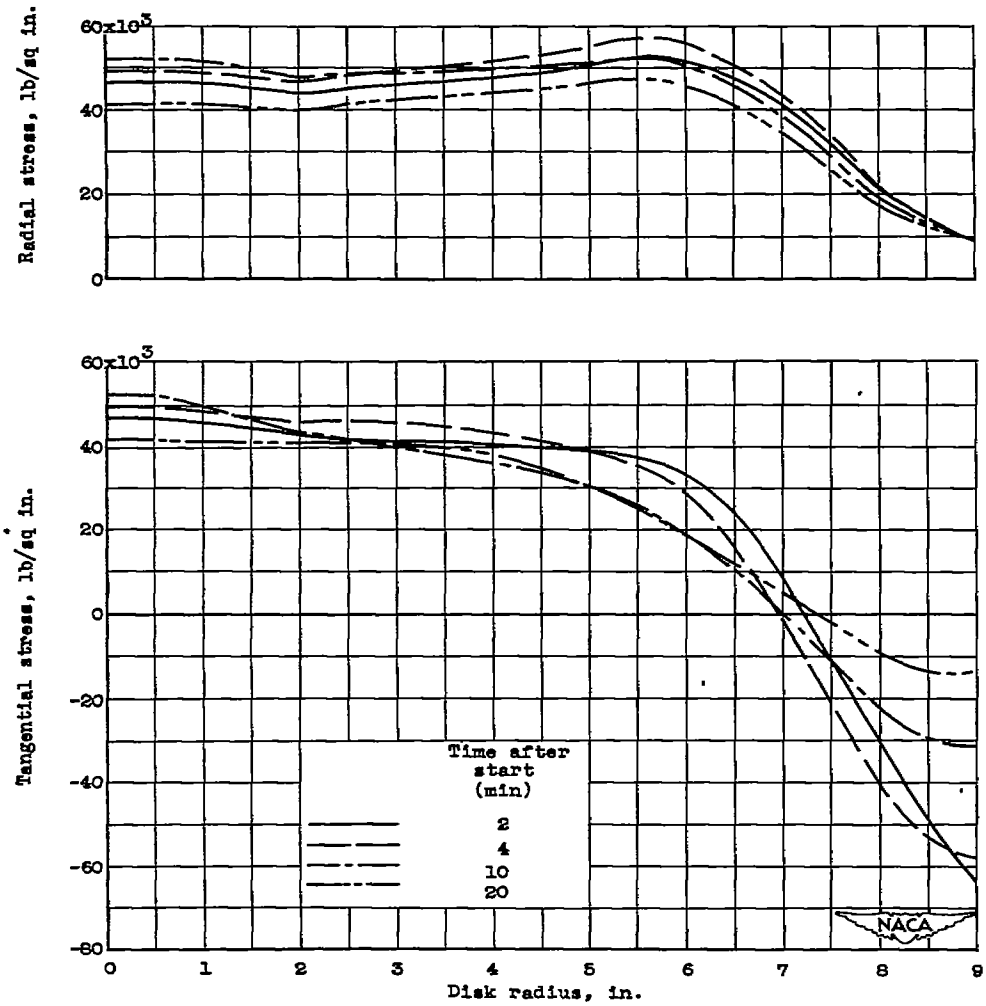

(c) Uncooled face of disk.

Figure 11. - Concluded. Plastic-stress distributions in turbine disk for various times during emergency take-off sequence.

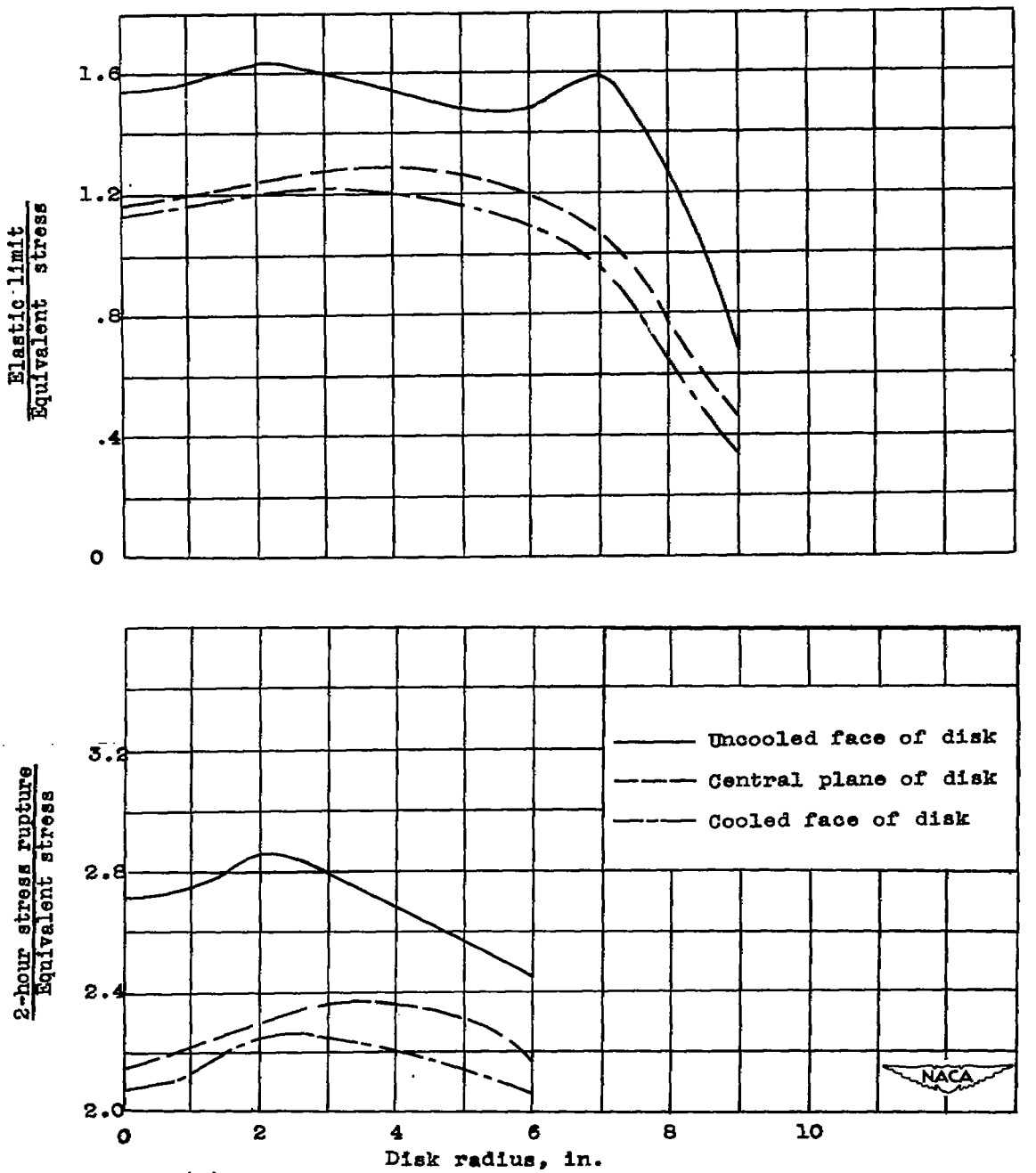

(a) After 16 minutes of typical take-off sequence.

Figure 12. - Flow and rupture criteria for turbine disk.

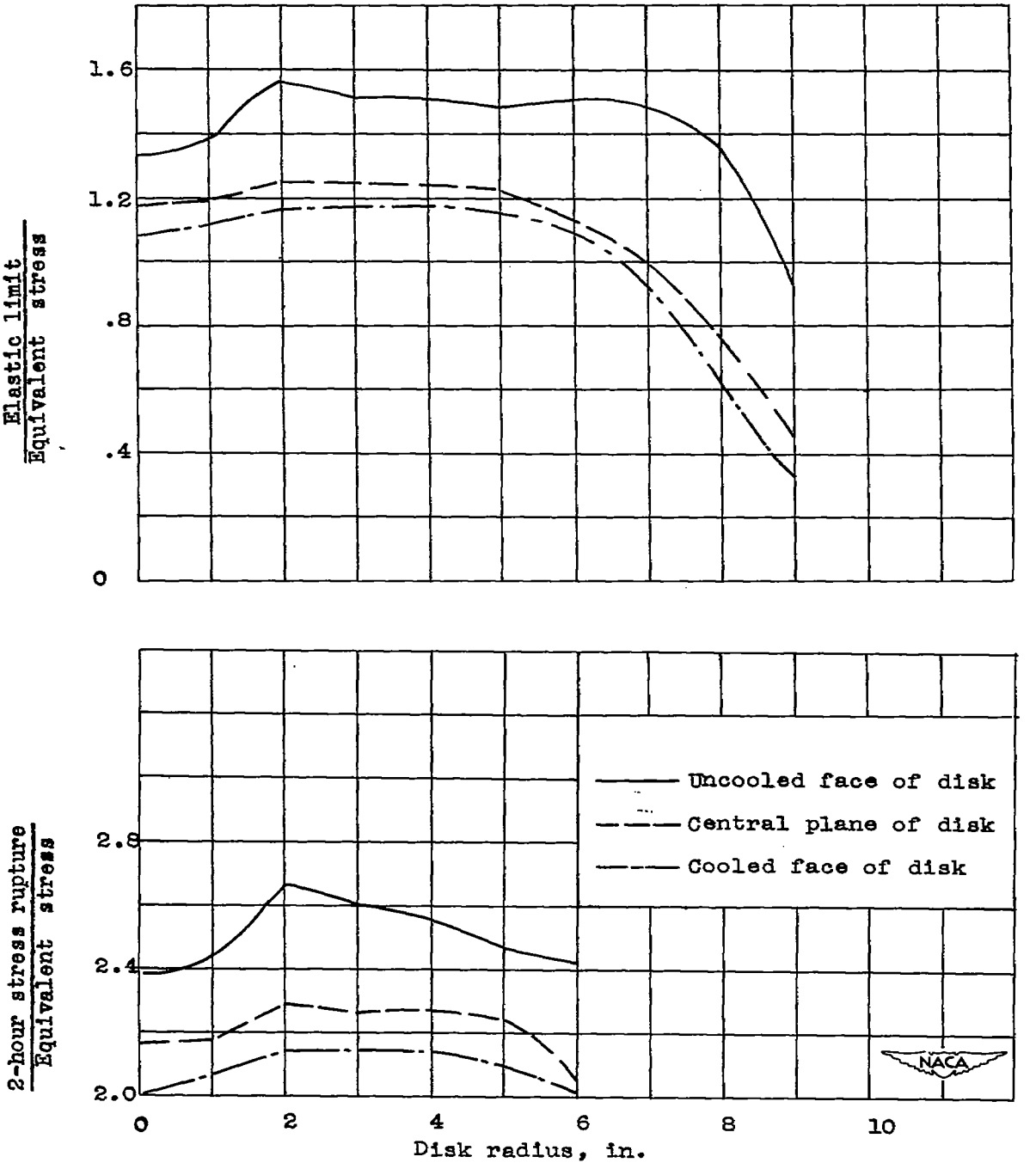

(b) After 10 minutes of emergency take-off sequence.

Figure 12. - Concluded. Flow and rupture criteria for turbine disk.

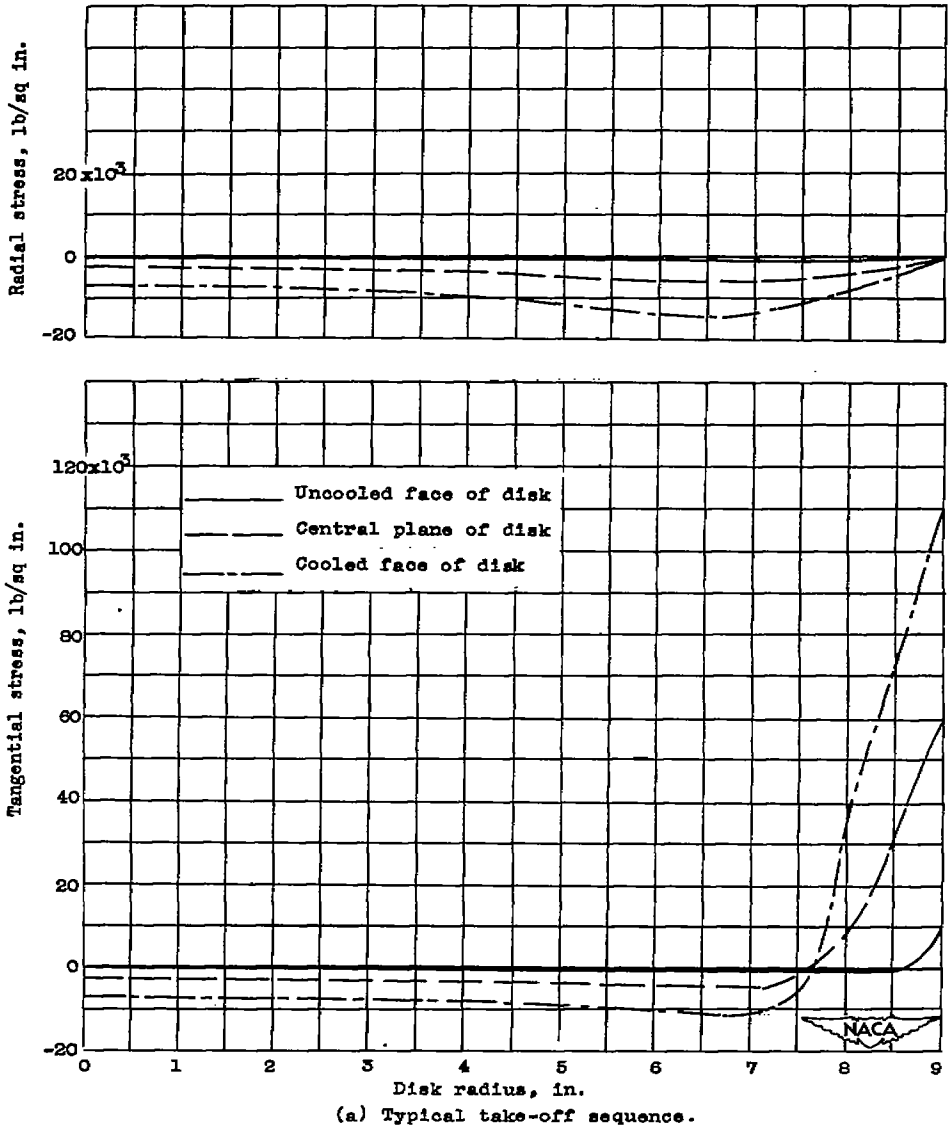

(a) Typical take-off sequence.

Figure 13. - Residual-stress distribution in turbine disk with welded blades after completion of take-off sequence.

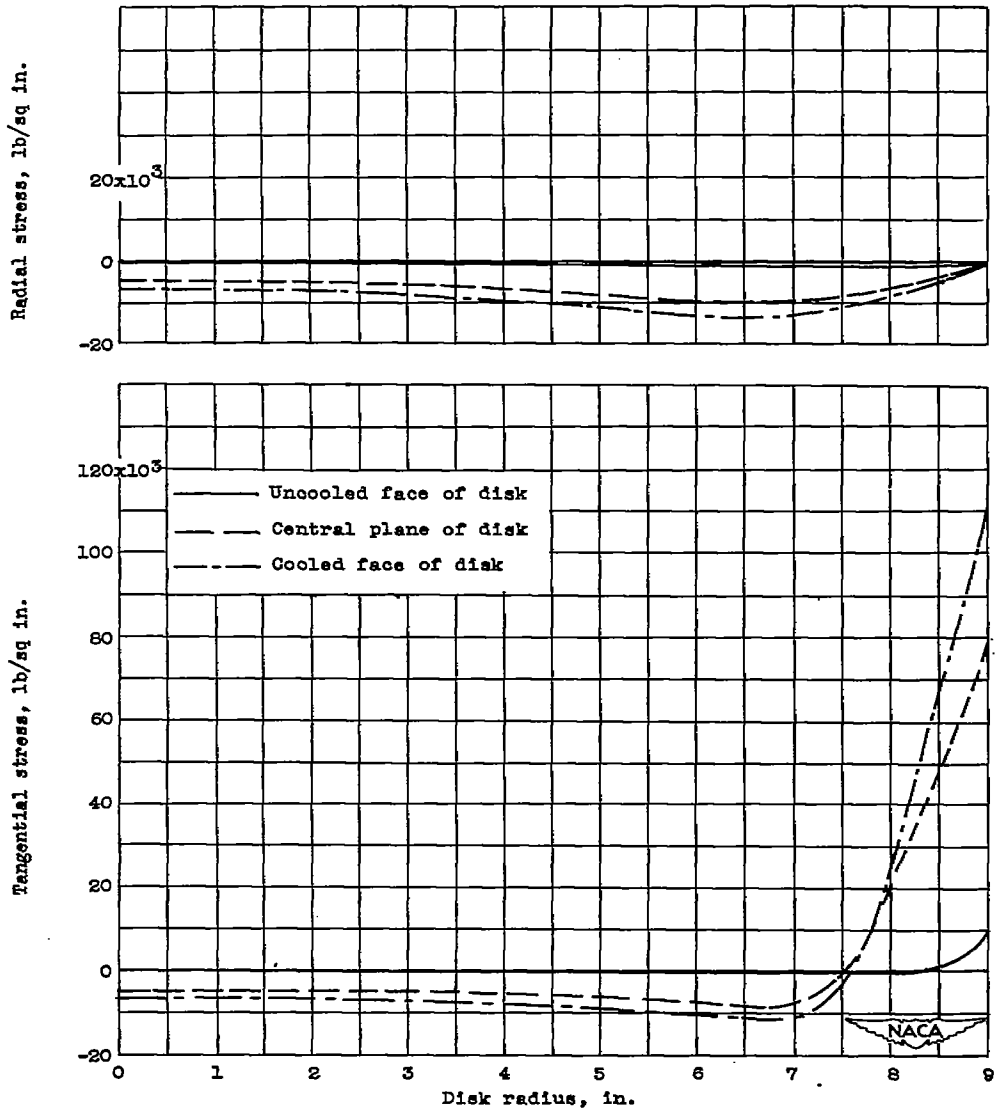

(b) Emergency take-off sequence.

Figure 13. - Concluded. Residual-stress distribution in turbine disk with welded blades after completion of take-off sequence.